ELSEVIER

Marine and Petroleum Geology 20 (2003) 861–882

Marine and Petroleum Geology

www.elsevier.com/locate/marpetgeo

Marine hyperpycnal flows: initiation, behavior and related deposits. A review

Thierry Mulder[a,*], James P.M. Syvitski[b], Sébastien Migeon[c], Jean-Claude Faugères[a], Bruno Savoye[d]

[a]*Département de Géologie et d'Océanographie, UMR 5805 EPOC, Université Bordeaux I, Avenue des Facultés, 33405 Talence cedex, France*
[b]*Department of Geological Sciences and Institute of Arctic and Alpine Research, University of Colorado, Box 450, Boulder, CO 80309-0450, USA*
[c]*Geological Survey of Canada Atlantic, Bedford Institute of Oceanography, P.O. Box 1000, Dartmouth, NS, Canada B2Y4A2*
[d]*IFREMER, DRO/GM, BP 70 29280 Plouzané, France*

Received 1 July 2002; accepted 9 January 2003

Abstract

Hyperpycnal flows form in the marine environment when river discharge enters the ocean with suspended concentrations in excess of 36 kg m^{-3} due to buoyancy considerations, or as little as 1–5 kg m^{-3} when convective instability is considered. They form at a river mouth during floods of small to medium size rivers including extreme events such as jökulhaups, dam breaking and draining, and lahars. Associated with high-suspended concentration, they can transport considerable volume of sediment to ocean basins. The typical deposit or hyperpycnite sequence is a compound of a basal coarsening-up unit, deposited during the waxing period of discharge, and a top fining-up unit deposited during the waning period of discharge. Hyperpycnites differ from other turbidites because of their well-developed inversely graded facies and intrasequence erosional contacts. These observations lead to a complete redefinition and interpretation of fine-grained turbidites. Hyperpycnite stacking can locally generate high-sedimentation rates, in the range of 1–2 m per 100 year. Because hyperpycnites are related to climate through flood frequency and magnitude, their record should vary with sea level and climate change. They can also be associated with proximal ice-melting settings. Hyperpycnal flows could also be involved in the formation of meandering canyons and channels.

Keywords: Hyperpycnal flows; River load; Canyon; Turbidite deposit; Floods; Climate

1. Introduction

In the past 30 years, offshore mass wasting processes and gravity flows have been widely studied, stimulated by the needs of deep-water reservoir characterization and other offshore industries needing protection against natural hazards. The importance of gravity processes is associated with new exploration of deep-marine environments including ODP drilling on the Amazon Fan (Hiscott, Pirmez, & Flood, 1997; Normark & Damuth, 1997) or industrial–academic surveys of the Zaire turbidite system (Savoye et al., 2000).

Following pioneer work of Kuenen and Migliorini (1950), early classifications of offshore gravity processes arose in the 1970s (Lowe, 1982; Middleton, 1976, 1993; Middleton & Hampton, 1973; Nardin, Hein, Gorsline, & Edwards, 1979). These classifications underlined the existence of two major processes in the marine environment: mass flows and turbidity currents. Mulder and Cochonat (1996) and Shanmugam (1996) discussed the complexity of a classification, since one single event may involve several processes from the failure to final deposition. Turbidity flows (Kneller & Buckee, 2000; Lowe, 1979, 1982; Middleton & Hampton, 1973, 1976; Nardin et al., 1979; Stow, 1996) result from slide transformation, continuation of a fluvial flow or concentration processes. Ignitive transformation of a submarine slide into a flow in which turbulent energy substantively increases (Emms, 1999; Fukushima, Parker, & Pantin, 1985; Parker, 1982; Parker, Fukushima, & Pantin, 1986) has been described worldwide, including the 1929 Grand Banks event (Hughes-Clarke, 1990; Hughes-Clarke, Shor, Piper, & Mayer, 1990; Piper, Cochonat, Ollier Le Drezen, Morrison & Baltzer, 1992), and the 1979 Nice event (Gennesseaux, Mauffret, & Pautot, 1980; Malinverno, Ryan, Auffret, & Pautot, 1988; Piper & Savoye, 1993).

* Corresponding author. Tel.: +33-556648845.
E-mail address: t.mulder@geocean.u-bordeaux.fr (T. Mulder).

0264-8172/$ - see front matter © 2003 Elsevier Ltd. All rights reserved.
doi:10.1016/j.marpetgeo.2003.01.003

Turbulent flow can also form by continuation at sea of river discharge (Normark & Piper, 1991), which is the aim of this paper. Advances include recognizing the importance of hyperpycnal flows from small and medium sized rivers (Mulder & Syvitski, 1995) and the use of digital X-radiography (Migeon, 2000; Migeon, Weber, Faugères, & Saint-Paul, 1999) to distinguish structures within fine-grained turbidites, particularly bed–intrabed contacts.

Turbulent flow initiation can also result of the intensification of the nepheloid layer circulation and density cascading (Mc Cave, 1986; Wilson & Roberts, 1995) or by formation of fluid-mud suspensions on continental shelves under storm conditions (Friedrichs, Wright, Hepworth, & Kim, 2000; Ogston, Cacchione, Sternberg, & Kineke, 2000; Reed, Niedoroda, & Swift, 1999; Traykovski, Geyer, Irish, & Lynch, 2000; Wright, Friedrichs, Kim, & Scully, 2001).

Bates (1953) defined hypopycnal flows as buoyant plumes flowing at the water surface and producing hemipelagites. They form when the density of particle–water mixture at the river mouth is less than the density of the basin it flows. Bates (1953) defined homopycnal flows as river effluent with a density in the same range as the density of the fluid in the receiving basin. These flows quickly decelerate and dump their particles, forming mouth bars with steep foresets between two water masses. Mulder and Alexander (2001) added mesopycnal flows, i.e. with an intermediate density. Such flows are observed in deep hypersaline basins with strongly stratified waters such as in the Mediterranean (Rimoldi, Alexander, & Morris, 1996) where they flow along a pycnocline.

Hyperpycnal flows were first reported by Forel (1885, 1892) in Lake Léman. They are frequent in Lake Mead (USA; Gould, 1951), Lake Baïkal (Russia; Nelson, Karabanov, Colman, & Escutia, 1999), and alpine lakes (Anterne, Annecy, le Bourget; Arnaud et al., 2001; Lambert, Kelts, & Marshall, 1976; Linier, 2001; Linier et al., 2001; Soper Lake, Baffin Island; Hughen, Overpeck, & Anderson, 2000). In lakes, the receiving basin is filled with fresh water and the density difference between effluent and basin water is low. In many mountain lakes, the streams result from ice or snow melting, with the temperature of the inflowing river water lower than the temperature of the ambient lake water. Plunging of the river effluent may form without any sediment in suspension although these rivers flows are usually accompanied by higher sediment concentrations. In rift lakes, suspended load is provided by the presence of easily erodible volcanic material such as ashes and pumice. Aerial views of Lake Tanganyika (Tanzania; Tiercelin, Cohen, Soreghan, Lezzar, & Bouroullec, 1992; Tiercelin et al., 1987) show the area on lake surface where the flow disappears (Fig. 1).

In the marine environment, river flow contributes to 95% of the global sediment flux delivered to the ocean from land by rivers (Table 1). Most of that flux is as suspended load (Syvitski, 2003).

Modifying slightly Bates definition, Mulder and Syvitski (1995) defined a hyperpycnal flow as a negatively buoyant flow that flows along the basin floor due to density in excess of ambient density of the standing water-body, as the result of the particle load that it carries. This implies that only suspended matter is concerned for a long-distance transport towards the deep-sea. This means that (1) hyperpycnal currents will transport distally only particles finer than medium sands and (2) sediment might be transported through a very long distance.

A hyperpycnal process means that riverine material, except what is eroded on the seafloor, is transported directly to the marine environment, the continental shelf and slope or to the abyss, by a turbulent flow initially containing fresh water. This definition of hyperpycnal flows excludes turbidity currents generated by slumps or foresets failures as those described by Bornhold, Ren, and Prior (1994), Mulder, Savoye, Syvitski, and Cochonat (1997b), Prior, Bornhold, and Johns (1986), Prior, Bornhold, Wisenam and Lowe (1987) or Zeng, Lowe, Prior, Wisenam, and Bornhold (1991) despite the correlation between record of turbidity currents and high river discharge.

In this paper, we review the conditions that generate hyperpycnal flows in the marine environment. They include seasonal floods or catastrophic extreme events such as jökulhaups, lahars, dam breaking and draining that can occur concomitantly with floods. We estimate how frequent hyperpycnal flows may form and how they can maintain their negative-buoyancy to transport large volume of particles in deep-sea environments. Finally, we describe the deposits that are related to hyperpycnal processes (hyperpycnites) and evaluate their importance in the explanation of margin morphology and the record of climatic changes in sedimentary series.

2. Hyperpycnal flows in the marine environment

2.1. Suspended sediment concentration at river mouth

Until recently, the existence of hyperpycnal flows in the marine environment has been contested. They have only been observed during unusually extreme conditions (jökulhaups and erosion of natural dams), and were reputed to be sporadic phenomena. Their initiation, i.e. the plunging at a river mouth necessitates high-suspended particle concentration in the fresh river water. The critical concentration for plunging (C_c) varies between 36 and 43 kg m^{-3} (Table 2), and depends on the temperature and salinity of seawater near the river mouth. Mulder and Syvitski (1995) provided average density threshold values for worldwide rivers depending on the climatic setting, i.e. the latitude of the river mouth.

In normal discharge conditions, the mean suspended concentration in rivers is low. Only nine rivers are ‘dirty’ in natural conditions, i.e. have a mean sediment concentration

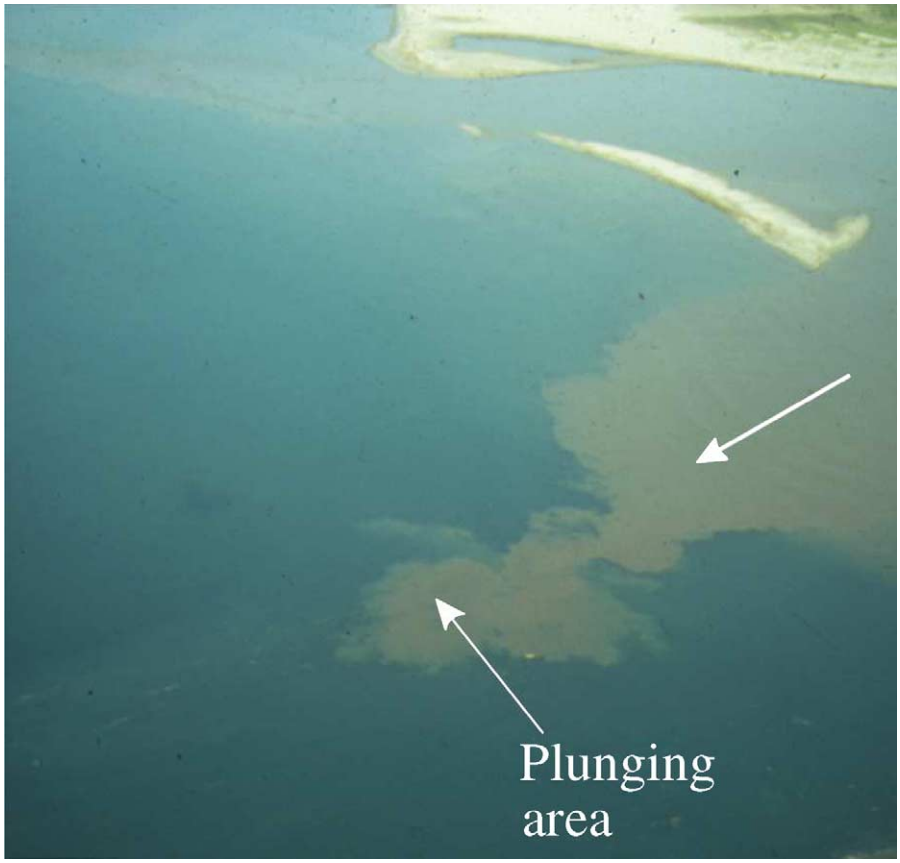

Fig. 1. Aerial photograph of hyperpycnal discharge in Lake Tanganyika (Tanzania; Tiercelin et al., 1987, 1992). The surface flow disappears at the plunging area, after which the current flows along the lake floor. The arrow shows flow direction. Photo courtesy of J.-J. Tiercelin.

to ensure frequent hyperpycnal flow initiation during a year (Table 3).

2.2. Flash floods in hot arid environments

Streams located in arid hot climates have an intermittent flow regime. The stream bed might stay dry during months or years. Water supply is sporadic, short and intense. North African 'oueds' are active after heavy rains (Isser and Djer rivers in Table 3). Californian and Mexican 'arroyos' flood after cyclones or hurricanes. Usually, these rivers build fan deltas at their mouth (Gorsline, de Diego, & Nava-Sanchez, 2000; Nava-Sanchez, Gorsline, Cruz-Orozco, & Godinez-Orta, 1999) that demonstrate the high discharges and flow velocities generated during flash floods.

A significant amount of the sediment is transported as suspended load and could generate hyperpycnal currents upon arrival at the coast. This is attested by the considerable erosion in stream beds on the continents (Fig. 2). Nava-Sanchez et al. (1999) observed turbidites in small anoxic basins around in the Gulf of California and supplied by Baja Californian streams. Some of the turbidites are

Table 1
Global estimates of the flux of sediment from land to the ocean (Syvitski, 2003)

Transport mechanism	Global flux estimate (10^{12} kg year^{-1})	Grade
Rivers: suspended load	18	B^+
Bed load	2	B^-
Dissolved load	5	B^+
Glaciers, sea ice, icebergs	2	C
Wind	0.7	C
Coastal erosion	0.4	D

Table 2
Average temperature, salinity (from Kennish, 1989) and density of seawater for different climates, and the corresponding critical particle concentration (C_c) to overcome difference between fresh and salt water assuming particle density of 2650 kg m^{-3}

	Temperature (°C)	Salinity (‰)	Density (10^{-3} kg m^{-3})	C_c (kg m^{-3})
(1)	27	34.75	1.02257	36.25
(2)	24	35.75	1.02424	38.93
(3)	13	35.25	1.02661	42.74
(4)	1	33.75	1.02708	43.49

(1) Equatorial (Lat. $<10°$); (2) Tropical and subtropical (Lat. 10–30°); (3) Temperate (Lat. 30–50°); (4) Subpolar (Lat. $>50°$). Modified from Mulder and Syvitski (1995).

Table 3
Dirty rivers that may produce one or several hyperpycnal flows each year

River	Q_{av} ($m^3 s^{-1}$)	$C_{s_{av}}$ (kg m^{-3})	C_c (kg m^{-3})
Choshui (Taiwan)	190	10.5	38.9
Djer (Algeria)	2	13.4	42.7
Tsengwen (Taiwan)	76	12.9	38.9
Isser (Algeria)	12	15.4	42.7
Rioni (Russia)	5	20.7	43.5
Daling (China)	38	36.0	42.7
Haile (China)	63	40.5	42.7
Huanghe (China)	1880	18.5	42.7
Erhian (Taiwan)	16	25.5	38.9

Average annual suspended particle concentration values (C_{sav}) is close to the critical threshold in concentration (C_c) to generate a hyperpycnal flow. Modified from Mulder and Syvitski (1995).

related to historical floods and may be deposited by hyperpycnal flows.

2.3. Jökulhaups in cold arid environments

'Jökulhlaup' is an Icelandic term meaning 'glacial flood'. Jökulhaups form under a glacier because of the melting of a large volume of ice. In Iceland, melting is due to a subglacial volcanic eruption. A subglacial lake forms. If the lake breaks through its confinement, millions of cubic meters of fresh water mixed with volcanic and glacial deposits flow to the ocean (Fig. 3). Jökulhaups last only a few hours. Such a jökulhlaup formed in November 1996 because of the eruption of the Grimsvötn volcano below the glacier Vatnajökull (Einarsson et al., 1997; Grönvold & Jóhannesson, 1984; Gudmunsson, Sigmundsson, & Björnsson, 1997). Peak discharge reached 50,000 $m^3 s^{-1}$ where the flow crossed the Skeidararsandur and reached the ocean after traveling <70 km. In two days, a total water volume of 3 km^3 including clay to boulders and ice blocks were transported to the ocean. During these jökulhaups, particle concentration is very high. The shortness of the phenomenon induces very high instantaneous discharges and flow velocities capable of transporting medium sand. Jorun Hardardottir (personal communication, 1997) reports sediment concentrations from this event reached 200 kg m^{-3}. When entering the sea, the flow plunges quickly (Fig. 3).

In non-volcanic areas covered by ice, jökulhaups form when a moraine dam is breached due to overpressuring, overflow or earthquake shaking.

2.4. Natural and artificial dam erosion

Natural dam erosion is well illustrated in the Saguenay Fjord, a tributary of the St Lawrence River (Fig. 4). This fjord is 93 km long, 1–6 km wide (Schafer, Smith, & Côte, 1990) and dissects the Laurentian Highlands of the Canadian Shield (Fig. 4). The Saguenay River drains the 78,000 km^2

Fig. 2. Erosion (arrow) of a stream bed after the hurricane Juliette in October 2001 (agua amarja, La Paz, Baja California, Mexico). The escarpment is approximately 3 m-high, located about 2 km from the river mouth.

Fig. 3. Aerial photograph of a hyperpycnal flow formation seaward of Skeidararsandur (Iceland) after the Grimsvötn eruption in November 1996 (photograph taken by Magnús Tumi Gumundsson and Finnur Pálsson (http://www.hi.is/~mmh/gos). The surface flow disappears quickly at the plunging point. Beyond this point, the current will flow along the Atlantic seafloor. Arrow indicates flow direction.

Lac-Saint-Jean basin, and flows into the head of the fjord (Fig. 4). In 1663 AD a high-magnitude earthquake occurred near the Saguenay Fjord and generated approximately 3 km^3 of landslides and submarine slides (Schafer & Smith, 1987; Fig. 5). Their deposits reached 100 m in thickness at some locations (Syvitski & Schafer, 1996). One of the terrestrial slides with a volume of 0.2 km^3 dammed the Saguenay River. The breach of the dam during the following spring facilitated a large flood reaching an estimated 9000 $m^3 s^{-1}$ peak discharge (Syvitski & Schafer, 1996).

A turbidite deposit 2–16 m thick, representing a volume of 0.31 km^3 (Figs. 4 and 5) resulted from the duration of the flood and high particle concentrations induced by erosion of the natural dam. Six hyperpycnites were deposited in the fjord during the last 7200 years (Saint-Onge, Mulder, Piper, Hillaire-Marcel, & Stoner, in press).

Artificial dams that break, such as the Malpasset Dam collapse (Bellier, 1967; Letourneur & Michel, 1971) in

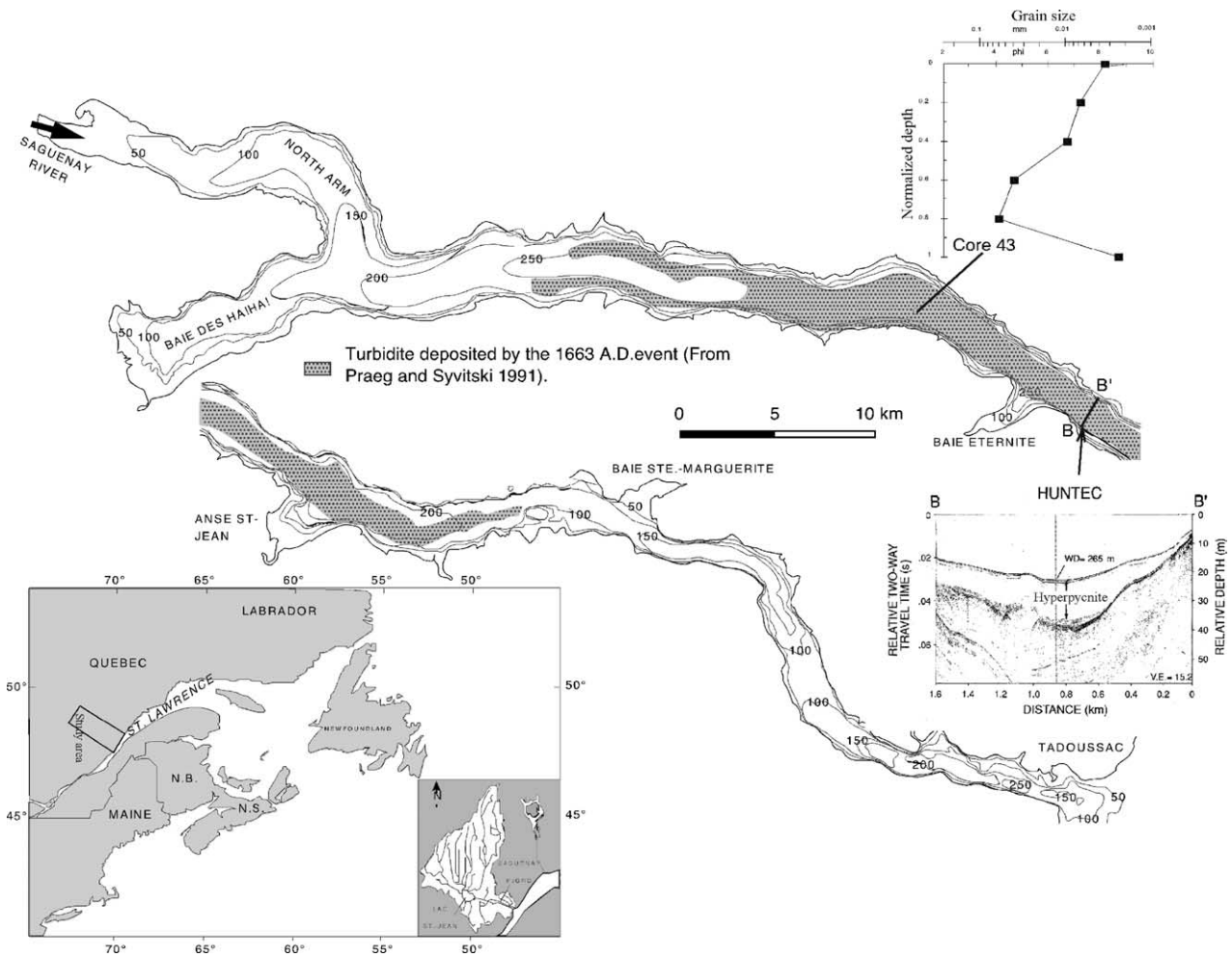

Fig. 4. Location map, bathymetry and extension of the 1663 AD turbidite deposits in the Saguenay Fjord. After Praeg and Syvitski (1991) and Syvitski and Schafer (1996). In inset, the grain size curve within the turbidite (from Mulder, Syvitski & Skene 1998b) and a very high-resolution (Huntec profile across debris flow deposits and the hyperpynal turbidite, both related to the 1663 AD earthquake-triggered slide and subsequent flood.

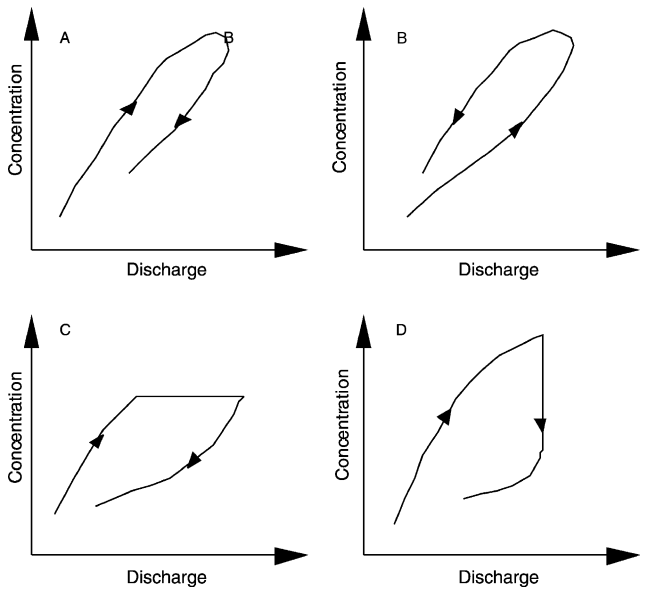

Fig. 5. Different shapes of a flood hydrograph. See text for details. Modified from Syvitski and Alcott (1995).

southern France in 1959, see their resulting catastrophic flow reach the sea and probably form a hyperpycnal flow. Power companies currently make controlled dam-draining to remove the fine particles that tend to accumulate at the toe of the dam. These drainings are associated with unusually high loads and form anthropic-controlled hyperpycnal flows. Such drainings are made frequently at the mouth of the Golo river on the eastern side of Corsica (French Mediterranean). They provide an excellent analogous experimental set-up of natural hyperpycnal flows.

2.5. Lahars transformation at sea

Lahars are concentrated or hyperconcentrated flows that form when heavy rainfall affects soft and underconsolidated volcanic pumice, ash or ignimbrites. When reaching the sea, lahars quickly dilute and transform into flows maintained for hours, creating a phenomenon similar to hyperpycnal flows.

However, these particular conditions do not need to occur to form a hyperpycnal flows. The most frequent way to trigger hyperpycnal flows is river flooding. Because flash floods, jökulhaups and lahars are all related to heavy rainfall, they tend also to be associated with floods. A key question is whether hyperpycnal flows can form without association with these extreme events?

3. Why do hyperpycnal flows form during a flood?

River particles are transported as bedload and suspended load (Emmett, 1982). Hyperpycnal flows are sediment-laden currents, thus we restrict the discussion to suspended load. There are two ways to predict suspended particle load and discharge at a river mouth: (1) by using a relationship between particle load and discharge deduced from measurements obtained regularly at the river mouth or (2) by using relationships linking particle load with morphologic parameters of the drainage basin.

Suspended load can be measured in rivers simultaneously with discharge. Today, the mean particle load of rivers under temperate climates is known during average discharge and flood conditions (Milliman & Meade, 1983; Milliman & Syvitski, 1992). However, intensification of artificial damming during recent decades reduced considerably the sediment load (Milliman & Syvitski, 1992) and hyperpycnal flow activity.

In addition, during a flood, the particle load always increases with discharge but this increase might be complex (Fig. 4; Syvitski & Alcott, 1993, 1995). First, the duration of the flood and the time to reach peak flow can take several hours to weeks (see examples in Mulder & Syvitski, 1995). Second, the particle concentration–discharge relationship can vary depending on the duration and intensity of the precipitation event. Particle concentration is usually higher during the rising limb of the flood hydrograph (Fig. 5a; e.g. the 1980 June flood of the Stikine River, Mulder & Syvitski, 1995). However, the opposite trend, i.e. particle concentration higher during the decreasing discharge period is also observed (Fig. 5b; e.g. the 1988 July flood of the MacKenzie River; Mulder & Syvitski, 1995). In some cases, depending on the availability of easily erodible particles, the concentration–discharge curve can show a plateau. The discharge continues to increase but the particle concentration remains constant (Fig. 5c; e.g. the 1980 July flood of the Stikine River, Mulder & Syvitski, 1995). Particle concentration can also decrease despite discharge that continues to increase or stabilize (Fig. 5d; e.g. the 1979 May flood of the Fraser River, Mulder & Syvitski, 1995).

All these complexities are solved by using the relationship between particle concentration and discharge (rating curve; Fig. 6) obtained from data measured daily or at higher frequency. For such return periods, rating curves are robust and usually allow valid predictions. Rating curves show suspended particle concentration (C_s) or load (Q_s) increases as a power relationship of discharge (Q). It can be written as follows:

$$Q_s = aQ^b \quad (1)$$

where a and b are the rating parameters that have to be measured in every river. The rating parameters can also be estimated from river basin characteristics (runoff, temperature, relief; Syvitski, Morehead, Bahr, & Mulder, 2000).

The shape of the rating curve demonstrates that:

- Hyperpycnal floods form during major floods. During major or extreme floods, a small increase in discharge induces a drastic increase in particle concentration.

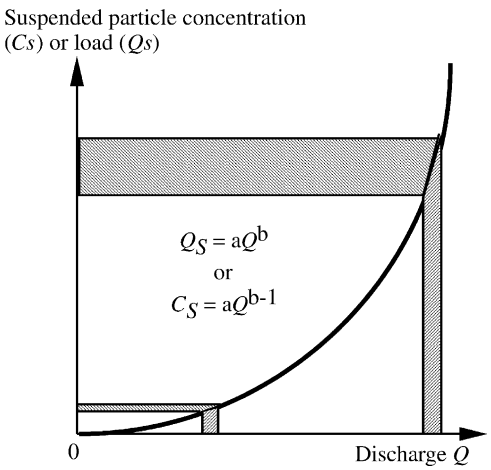

Fig. 6. The rating curve: power-law relationship between particle concentration, C_s and discharge, Q. During low-discharge periods, a small increase in discharge leads to insignificant increase in particle load. During high discharge periods the same increase in discharge induces a drastic increase in particle load.

- Hyperpycnal floods are of major interest because of the total volume of sediment they carry. During a major flood lasting days, river can transport as much sediment to its mouth as during the preceding years to decades.

For example, in November 1994, the Var River in the western Mediterranean had a major flood that lasted 3 days. During this bicentennial flood, the peak discharge reached almost 4000 $m^3\ s^{-1}$ (mean annual discharge at the Var river mouth is 52 $m^3\ s^{-1}$). Mulder, Savoye, Piper, and Syvitski (1998a) estimated that the flood generated a 18 h-long hyperpycnal flow. During this period, the hyperpycnal flow carried 11–14 times the mean annual particle load. The whole flood probably carried the same amount of material as during the preceding 20 years.

The importance of hyperpycnal floods as a sediment transport process may be underestimated for many rivers. The monitoring of peak flood conditions is important to generate an accurate rating curve and remains a challenge of future research. With hostile conditions, extreme events are usually not monitored biasing published data toward non-peak discharge conditions. Empirical relationships exist between discharge, particle load and morphology of the drainage basin. For example the mean annual discharge of a river is related to the surface of the drainage basin or the length of the river (Hack, 1957; Mulder & Syvitski, 1996). The relationship is better when climatic parameters are included in the relationship. There is good correlation ($r^2 = 0.9$) between the observed discharge of a river and its potential discharge (precipitation across the slope-adjusted drainage area). More importantly, the maximum limit of discharge (Q_{flood}) a river can experience at its mouth is very well correlated with the drainage area (Matthai, 1990).

The best general relationship to estimate sediment load is from Morehead, Syvitski, Hutton, and Peckham (2003) and Syvitski (2002):

$$\bar{Q}_s = \alpha H^{3/2} A^{1/2}\, e^{k\bar{T}} \quad (2)$$

where H is river basin relief (m), A is river basin area (km^2), $\bar{T}$ is mean surface temperature of the drainage basin (°C), and α is a dimensionless constant (2×10^{-5}) as is k (0.1331).

4. Hyperpycnal flow as a common process in the marine environment

4.1. Statistical analysis of hyperpycnal flow initiation by rivers

Mulder and Syvitski (1995) published tables for 147 rivers, listing the load-averaged mean concentration of suspended sediment, $\bar{C} = Q_s/Q$, calculated from a global database of mean annual river discharge Q and sediment discharge Q_s. The database accounts for 65% of the global particle load carried by rivers (Table 4). Because sediment transport is a highly nonlinear process (Garcia & Parker, 1993), flood values of $\bar{C}$ may deviate significantly from the annual mean. To account for this, Mulder and Syvitski (1995) use the sediment rating curve Eq. (1). Using rating curves, a drainage-area–maximum-flood relation, and a critical sediment concentration C_c of approximately 42 kg m^{-3}), Mulder and Syvitski (1995) classified rivers according to their capacity to generate a hyperpycnal flow. First, rivers with $C_c \leq 5\bar{C}$ were said to be dirty, and could reasonably produce a hyperpycnal flow every year due to seasonal variations (assumed to be a factor of five) in sediment discharge. Only 9 out of the 147 rivers could be called dirty and most were small rivers draining mountainous terrain. The other rivers were categorized by calculating a maximum flood discharge Q_{flood}. Taking the ratio of the flood and mean annual sediment rating curves, yields the expression:

$$C_{flood} = \bar{C}(Q_{flood}/Q)^b \quad (3)$$

The exponent b was varied until $C_{s_{flood}} > C_c$. Depending on the b required to produce $C_{s_{flood}} > C_c$, the return period of hyperpycnal flow formation was inferred. Small, easy-to-attain values of b were related to short return periods, while

Table 4
Change in the characterization of rivers when the influence of convective instability is considered

Criterion	(1)	(2)	(3)	(4)	(5)
$C_{mass} = 42$ kg m^3	9	72	24	13	29
$C_{mass} = 5$ kg m^3	61	48	15	8	15

The 147 rivers discussed in Mulder and Syvitski (1995) were reanalyzed using a criterion for hyperpycnal flow generation corresponding to that for sediment-driven convection. River categorization: (1) dirty; (2) moderately dirty; (3) moderately clean; (4) clean; (5) hyperpycnal activity not possible.

large b values were indicative of relatively rare events. The method provides a simple, rational way to classify rivers with limited data. The classifications were defined as follows: $b \leq 1$, moderately dirty (return periods of less than 100 years); $1 < b \leq 1.5$, moderately clean (return periods on the order of hundreds of years); $1.5 < b \leq 2$, clean (a return period on the order of tectonic/climatic time scales); $b > 2$, unlikely to ever produce a hyperpycnal flow.

Using these definitions, Mulder and Syvitski (1995) demonstrated that 81 rivers (55%) can produce >1 hyperpycnal flood every 100 years, and another 24 rivers can produce hyperpycnal flows every 100–1000 years. Thus 71% of the rivers in the database can generate hyperpycnal flows in the marine environment with a high to moderate frequency. Among the remaining rivers, only 29 are unlikely to ever produce hyperpycnal flows while 13 other rivers may produce hyperpycnal flows at a frequency of one every 1000–10,000 years.

4.2. Specific conditions increasing the frequency of hyperpycnal flow formation

Discovery of hyperpycnal flow-related sedimentary sequences in the Zaire deep-sea fan (Migeon, 2000) even though the Zaire was classified as a clean river (Table 5) suggests hyperpycnal flows may be more common than that suggested by Mulder and Syvitski (1995).

Table 5
Sample of world rivers that cannot produce hyperpycnal flows

River	Q_{av} ($m^3\ s^{-1}$)	$C_{s_{av}}$ ($kg\ m^{-3}$)	C_c ($kg\ m^{-3}$)	$C_{s_{flood}}$ ($kg\ m^{-3}$)
Orinoco (Ven)	34,500	0.14	36.2	<1
Mississippi (USA)	15,500	0.8	42.7	11
Amazon (Bra)	17,500	2.0	36.2	14
Paraná (Arg)	13,600	0.18	38.9	3
Columbia (USA)	7960	0.06	42.7	2
Mekong (Viet)	14,800	0.3	38.9	4
Danube (Rom)	6420	0.3	42.7	25
Yukon (USA)	6120	0.3	42.7	26
Zambezi (Moz)	17,600	0.09	38.9	<1
MacKenzie (Can)	9750	0.14	43.6	4
Amur (Rus)	10,600	0.16	42.7	4
Zaire (= Congo) (Zaï)	41,200	0.03	36.2	<1
Pechora (Rus)	3370	0.06	43.6	13
Niger (Nig)	6140	0.21	36.2	17
Volga (Rus)	17,200	0.03	42.7	0.4
Ob (Rus)	10,300	0.05	43.6	1
Lena (Rus)	16,200	0.02	43.6	0.3
Yenisey (Rus)	18,000	0.02	43.6	0.2
S. Dvina (Rus)	3660	0.04	43.6	8
Kolyma (Rus)	2840	0.07	43.6	25
Sao Francisco (Bra)	3040	0.06	36.2	21
St Lawrence (Can)	14,900	0.01	42.7	0.1

The maximum flood concentration in suspended particle, $C_{s_{flood}}$ is calculated using $C_{s_{flood}} = C_{s_{av}}(Q_{flood}/Q_{av})^b$ with $b = 2$. It is always below the concentration threshold (C_c) to generate hyperpycnal flows (Mulder & Syvitski, 1995). $C_{s_{av}}$, average annual suspended particle concentration values; Q_{av}, average annual discharge values.

The critical concentration for initiation of hyperpycnal flows can be considerably reduced by convective instability of a hyperpycnal flow (Hoyal, Bursik, & Atkinson, 1999; Maxworthy, 1999). The Chikita (1991) model and Parsons, Bush, and Syvitski (2001) experiments have demonstrated hyperpycnal flows to be generated with sediment concentrations 40 times less than those required to render the outflow heavy relative to the oceanic ambient (i.e. 1 $kg\ m^{-3}$). During the experiments of Parsons et al. (2001), convection took the form of sediment-laden fingers descending from the base of the surface flow. At 5 $kg\ m^{-3}$, finger convection is at least as vigorous as observed floc settling and can generate convection for any realistic, stabilizing temperature stratification. Lowering the critical threshold C_c from 42 to 5 $kg\ m^{-3}$, and using the same logic as Mulder and Syvitski (1995), 61 rivers are likely produce hyperpycnal flows annually (Table 3). Most of the rivers previously characterized as 'moderately dirty' are now characterized as dirty; among these are the Eel River and the larger rivers of New Zealand and Taiwan. The 61 rivers, now characterized as dirty, produce 53% of the world's oceanic sediment load, and are therefore responsible for a significant portion of the global sediment record. This new analysis suggests that 84% of the rivers in the database can generate hyperpycnal flows in the marine environment with a frequency of more than one event every 100 years.

In addition to convective instability several factors can reduce the density threshold necessary to generate plunging.

- *Specific geological setting*. There are some areas in the world covered by extensive soft and easily erodible deposits, such as the wind-transported loess in China (Daling, Haile or Huanghe, Table 2). The loess is intensively eroded during the monsoon rains, generating unusual suspended particle concentration at river mouths. These rivers generate several month-long hyperpycnal flows as recorded by Wright et al. (1986, 1988, 1990). In a similar way, easily erodible black shales in Alps may account for hyperpycnal flow formation at the Var river mouth.
- *Extreme geologic events* as jökulhaups, lahars, dam breaking or draining can create unusual fine-particle load and generate hyperpycnal flows in clean rivers, as illustrated by the Saguenay example.
- *Dilution of sea-water by fresh water during long-duration floods* can decrease the concentration threshold to initiate hyperpycnal flows. Examples include restricted narrow basins such as fjords or canyons or monsoon-triggered floods of Asian rivers.
- *Erosion of mouth bars*.

Conversely, natural processes such as coastal upwelling may locally increase the critical threshold for initiation of hyperpycnal flows. In areas submitted to strong winds moving from the continent to the ocean, warm surface sea-water is transported seaward and replaced by denser deep

water. This phenomenon occurs for example in south of France during southward Mistral winds.

4.3. River size versus hyperpycnal flow initiation

Rivers that can generate hyperpycnal flows are small to medium-size with an average annual discharge $<380-460\ m^3\ s^{-1}$. The ability to produce hyperpycnal flows increases with high relief (Milliman & Syvitski, 1992). Steep slopes are observed in tectonically active basins where flood-related deposits are frequent (Mutti, Davoli, Tinterri, & Zavala, 1996; Mutti, Ricci Lucchi, & Roveri, 2000).

The Var River is a type river that produces hyperpycnal flows. It is 120 km-long and connects directly into a sinuous steep submarine canyon that feeds a 20,000 km^2 deep-sea fan in the Mediterranean Sea. Flash floods generated by violent storms during spring or autumn erode black shales, providing fine suspended particles (Mulder et al., 1998a). Statistical analysis using river discharge and rating curves show that the Var can produce hyperpycnal floods with a frequency of one every 2–5 years (Mulder, Savoye, Syvitski, & Parize, 1997c).

Conversely, 'Giant' rivers, i.e. rivers with an average annual discharge more than 500 $m^3\ s^{-1}$ such as the Nile, the Mississippi and all the Siberian rivers have maximum flood particle concentrations far below the concentration threshold that would generate hyperpycnal flows (Table 5). Two reasons, in addition to sediment availability, explain the inability for large rivers to form hyperpycnal flows. First, their particle concentration is diluted by their considerable volume of water. Second, giant rivers trap much of their sediment load within their flood plains and subaerial deltas. In the case of the Amazon, 20% of its annually delivered load (10^{12} kg $year^{-1}$) is retained within its delta; the remaining 80% is deposited on the continental shelf and coast with none reaching the deep sea. In the case of the Ganges and Brahmaputra Rivers, 55% of the annual load (1.1×10^{12} kg $year^{-1}$) is retained within its delta; the remaining 45% is deposited on the continental shelf and coast (36%) with 9% reaching the deep sea.

In the case of the Huanghe, 82% of the annual load (1.1×10^{12} kg $year^{-1}$) is retained by its delta; the remaining 18% is deposited on the continental shelf and coast (36%) with none reaching the deep sea (Meade, 1996).

5. Hyperpycnal flow motion

5.1. How do hyperpycnal flows plunge?

Turbidity currents generated at the river mouth consist of three distinct parts (Kassem & Imran, 2001): the plunge region, the main body, and the leading head. Each part of the current has distinct characteristics and plays an important role in the overall flow and transport processes (Kassem & Imran, 2001). The ambient-water entrainment during plunging affects the rest of the current. Vertical structures of sediment concentration and velocity in the main body of the current are responsible for sustained scour of and deposition on the basin floor. The mixing at the leading head determines how far the current may travel before it loses its identity. Various factors such as flow Richardson and Reynold numbers, bottom slope of the basin, and confluence divergence angle influence the plunging process including the plunge depth and location and subsequent evolution of the current.

Only few attempts have been made to model the plunging process and subsequent generation of hyperpycnal flow in its entirety (Akiyama & Stefan, 1984, 1988; Bournet, Dartus, Tassin, & Vincon-Leite, 1999; Farrell & Stefan, 1989). The numerical model used by Kassem and Imran (2001) successfully predicts the development of the entire process from the free-surface-flow condition at the upstream end to the formation of the turbidity current including the stabilization of the plunge point. As the sediment-laden water flows in with a dominant dynamic force, the reservoir water is pushed forward and a separation surface becomes pronounced. When the pressure force at the bottom becomes significant, it accelerates the flow at the bottom at a rate higher than the movement at the top. As the pressure forces continue to grow, the flow plunges to the bottom and begins to move as an underflow. At this stage, the velocity at the top surface is still significant enough to move the plunging point forward. When the equilibrium is reached, the velocity at the top disappears, and a stable plunge point (plunge line in a 3D flow) forms and the current moves forward with a bulge-shaped head and an elongated body.

The Eel River (Northern California) is a study area where hyperpycnal flow formation has been modeled and constrained by field data. The Eel margin extends from Cape Mendocino to Trinidad Head in northern California. It drains a 9400 km^2 basin but has the highest particle yield for rivers of similar or larger size in the conterminous USA (Brown & Ritter, 1971; Milliman & Syvitski, 1992). It discharges on a narrow (10–20 km-wide) continental shelf and is one of seven rivers located in the United States that can produce hyperpycnal flow during a 100-year flood event. The river experienced such a flood in 1964 and possibly in 1995 and 1997. Surveys conducted by investigators of the ONR STRATAFORM program (Nittrouer, 1999) immediately after the 1995 flood revealed that only ~25% of the flood sediment discharged by the Eel River remained on the shelf (Wheatcroft et al., 1996, 1997). Storm-induced currents may play a role in resuspending and transporting some of the flood sediment as fluid-mud suspensions traveling across the shelf as density currents (Mullenbach & Nittrouer, 2000; Scully, Friedrichs, & Wright, 2002; Sommerfield & Nittrouer, 1999; Sommerfield, Nittrouer, & Alexander, 1999; Wheatcroft &

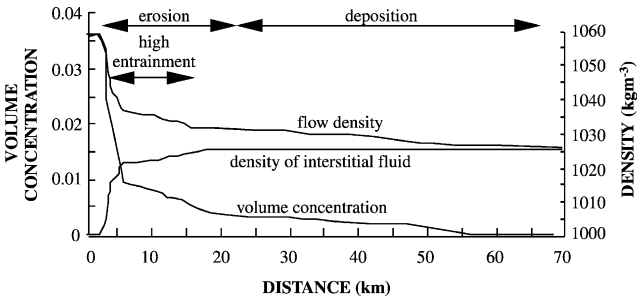

Fig. 7. Synthetic curves showing the modeled evolution with distance of volume concentration, density of interstitial fluid and flow density with distance for the 1663 Saguenay hyperpycnal flow (Mulder et al., 1998b).

Borgeld, 2000). Hyperpycnal flows may play the dominant role during the peak flood condition. The flow may travel towards the adjacent Eel Canyon and deliver sediment to the base of the continental slope. In the presence of long shelf currents, the head of the turbidity current is turned away from the canyon (Imran, Parker, & Katopodes, 1998; Imran & Syvitski, 2000).

5.2. How are hyperpycnal flows maintained on the seafloor?

When hyperpycnal flows form at a river mouth, they plunge because of high suspended concentrations possibly aided by convective instability. During transport, suspended particles begin to settle and particle concentration will decrease. If the excess density is not maintained, the hyperpycnal flow may disconnect from the seafloor, and flow as a water mass within the ocean's general circulation.

Mulder, Syvitski, and Skene (1998b) and Skene, Mulder, and Syvitski (1997) have modeled several field cases of marine hyperpycnal flow. They showed that a hyperpycnal flow is maintained along the seafloor because: (1) entrainment of sea-water into the flow progressively increases the density of the water phase while dilution of the suspended particle concentration decreases the internal friction and (2) erosion of the seafloor increases flow density (driving force). Along the travel path of the 1663 AD Saguenay event, density of the modeled interstitial fluid reached 1020 kg m^{-3} at 5 km from the river mouth and 1027 kg m^{-3} (i.e. the density of the ambient ocean water) at 22 km where deposition began (Fig. 7).

5.3. Differences with slide-induced flows

Hyperpycnal flows have several particularities that make their hydrodynamic behavior different than the behavior of turbulent surges (Ravenne & Beghin, 1983) that results of the transformation of slides or debris flows (Table 6).

In hyperpycnal flows, the initial internal fluid is fresh water. This necessitates the maintenance of negative buoyancy by suspended sediment for plunging. The driving force responsible for the downward motion is likely smaller for a hyperpycnal flow than for a slide-induced flow. In a hyperpycnal flow, the initial particle concentration is lower than for a turbulent surge. As shown in Fig. 7, particle concentration remains above the critical threshold but is never very high (42–100 kg m^{-3}). The threshold (42 kg m^{-3}; Table 1) is equivalent to a volume concentration of 1.5%, well within the criteria for autosuspension (volume concentration $<9\%$; Bagnold, 1962). In a slide-triggered flow, the initial flow density is closer to the density of the in situ sediment at the initial failure location (1300–1700 kg m^{-3}). After slide initiation, the particle concentration rapidly decreases due to fluid entrainment. The flow transforms into a hyperconcentrated or concentrated flow. In some cases, because the original fluid is already dense salt water, surge turbidity currents can maintain a driving force with very low particle concentration i.e. a few kg m^{-3}. This is the case for the flows recorded by Gennesseaux, Guibout, and Lacombe (1971) in the Var Canyon (Mulder et al., 1997b). Such low concentrations can also be observed in hyperpycnal flows but only in the most distal part of their travel, when the interstitial fluid density substantially increases because of water entrainment (Table 6).

The initial presence of fresh water in hyperpycnal flows will strongly reduce the density difference between flow and ambient water. As demonstrated in laboratory hyperpycnal flows (Alexander & Mulder, 2002) hyperpycnal flows are largely slower than turbulent surges moving on the same slopes. Numerical modeling of the slide-generated turbulent surge that affected the Var canyon in 1979, and the 1663 AD hyperpycnal flow in the Saguenay fjord, also highlight this difference. The velocity of the 1979 Var surge is estimated to have reached 30–40 m s^{-1} in the upper part of the canyon, and 5–10 m s^{-1} in the middle fan valley (Mulder, Savoye, & Syvitski, 1997a; Piper & Savoye, 1993). The Saguenay flow reached 2 m s^{-1} but more typically flowed at <1 m s^{-1} over its travel path.

Hyperpycnal flows can be described as slow, turbulent, flows with their density largely remaining low along their

Table 6
Behavior of hyperpycnal and slide-induced flows

Hyperpycnal flows	Surge-induced flow
Minimum threshold of particle concentration for triggering	No minimum threshold of particle concentration for triggering
Initial concentration: 5(?)–200 kg m^{-3}	Conc: <1–1500 kg m^{-3}
Flow velocity: <2 m s^{-1}	Flow velocity: <4 m s^{-1} >10 m s^{-1} on steep slopes
Thick and long flow. No individual flow head	Thick flow. Well-defined flow head, body and tail
Quasi-steady flows	Unsteady flows
Duration: minutes to weeks	Duration: minutes to hours

Synthesis of in situ observations (Gennesseaux et al., 1971), laboratory experiments (Alexander & Morris, 1994; Alexander & Mulder, 2003; Garcia, 1994; Garcia & Parker, 1984, 1989; Laval et al., 1988; Luthi, 1981; Middleton, 1967; Mulder & Alexander, 2001; Ravenne & Beghin, 1983), and numerical modeling (Mulder et al., 1998b; Skene et al., 1997).

travel path. They fit the description of the 'low-density turbidity currents' of Lowe (1982), Mulder and Cochonat (1996), and Nardin et al. (1979). Conversely, slide-induced surge turbidity currents represent the transformation of fast moving flows through ignition (Emms, 1999; Parker, 1982). The high velocity is due to the initial driving force and possibly the reduction of basal friction through hydroplaning (Mohrig, Whipple, Hondzo, Ellis, & Parker, 1998). In this series of transformations, flow concentration and density both constantly decrease due to water entrainment. Most of the members of this style of flow are regarded as the 'high-density turbidity currents' of Lowe (1982), Mulder and Cochonat (1996), and Nardin et al. (1979). This highlights the meaning of the term 'hyperpycnal'. Hyperpycnal means 'above a density threshold' and not 'high density'.

- Surge-type turbidity currents have a strong concentration gradient (Kneller & Buckee, 2000; Stacey & Bowen, 1988). This suggests that base and top of the flow can behave differently. Hyperpycnal flows have a more gradual vertical gradient in particle concentration (Mulder & Alexander, 2001).
- Hyperpycnal flows are quasi-steady (Mulder & Alexander, 2002). That means their velocity increases and decreases slowly with time. This characteristic is related to their flood origin, i.e. an event during which both river discharge and velocity increase, pass through a peak, and then decrease. As a strong part of the discharge increase includes changes in river depth and width, river velocity increases more slowly than river discharge. Quasi-steadiness allows more simple numerical models to be applied to hyperpycnal flows. Turbulent surges which are typical unsteady flows that accelerate shortly after the triggering and then decelerate rapidly require more complex models (Pratson, Imran, Hutton, Parker, & Syvitski, 2001).

6. Flood-related deposits

6.1. Hyperpycnal flow deposits: hyperpycnites

The type-hyperpycnal sequence is defined by Mulder, Migeon, Savoye, and Faugères (2001a) (Fig. 10a and b). To avoid misunderstanding between flow deposits and their hydrodynamic behavior, Mulder and Alexander (2001) restrain the term 'turbidite' to deposits from true turbidity currents, i.e. currents in which support of suspended particles is mainly due to turbulence. Hyperpycnal sequence belongs to this category and their related deposits are turbidites. The sedimentary sequences deposited by surge turbidity currents are significantly different from turbidite beds or 'hyperpycnites' resulting from hyperpycnal flows (Mulder, Migeon, Savoye, & Faugères, 2002). The complete sequence is explained by the shape of the flood hydrograph and predicted by the acceleration matrix of Kneller (1995) and Kneller and Branney (1995) (Fig. 8).

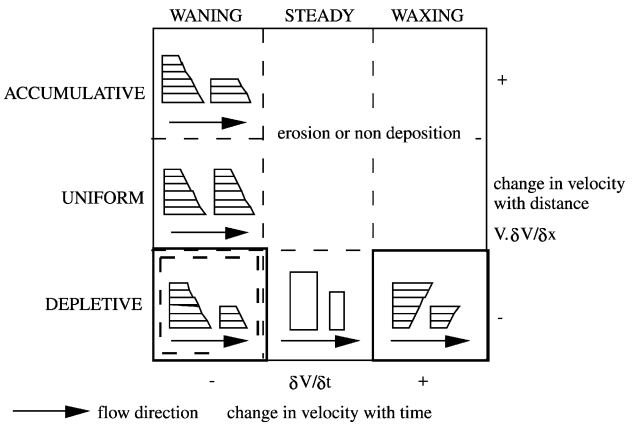

Fig. 8. The acceleration matrix from Kneller (1995) and Kneller and Branney (1995). The predicted Bouma sequence resulting from the deposition of a waning surge is dashed. Plain lines circle two stacked units of a hyperpycnite: the basal coarsening-up unit deposited by a waxing flow and the top fining-up unit deposited by the waning flow.

During the increasing or waxing discharge period at the river mouth, the hyperpycnal flow will develop a coarsening-up basal unit, Ha (Figs. 9 and 10; Mulder et al., 2001a). During the decreasing or waning discharge period at the river mouth, the hyperpycnal flow will deposit a fining-up top unit, Hb (Figs. 9 and 10). The complete hyperpycnite is these two stacked units (Figs. 8–10a, b). The Ha–Hb transition corresponds to the maximum grain size and marks approximately the peak of the flood, i.e. the period of maximum energy (discharge) at the river mouth, except when the flood hydrograph shows a plateau in discharge of particle concentration (Fig. 5c and d).

Bourcart (1964) described cores from the Var system containing similar beds with grain size first increasing from silt to sand and then decreasing to silt. In addition to these two units, a typical hyperpycnite contains sedimentary structures that are attributed to ripple migration (Fig. 10a and b). The most common structures are climbing ripples (Migeon et al., 2001; Mulder et al., 2002; Mutti et al., 2002 and this volume), which suggests particle deposition larger than particle transport. The presence of both sedimentary structures and a clear sorting suggest that the flows are low-concentrated and that particle settling and traction acts simultaneously. Hyperpycnites show laminae that represent hydrodynamic fluctuation in the bottom boundary layer of a single turbulent flow (Hesse & Chough, 1980). Bourcart (1964) noted that the sand-silt-sand beds in the Var system contained abundant organic matter with *Chara* oogoniums and abundant leaves of continental species. These occurrences suggest a continental source for much of these sediments. Linier (2001) and Linier et al. (2001) noted that evolution of grain-size parameters (sorting, mode, asymmetry) show a different vertical evolution in hyperpycnites and in sequences deposited from slide-triggered turbulent surges.

Pulses of the hyperpycnal flow due to variations in the flood hydrograph could be at the origin of minor intrasequence erosion at the base of coarse fine laminae

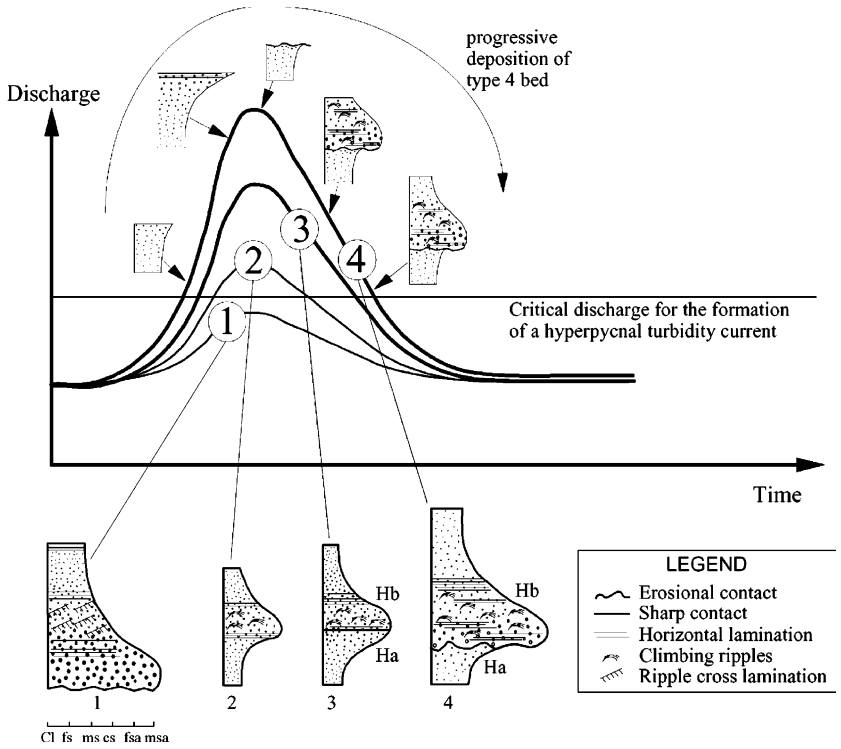

Fig. 9. Facies and sequences deposited as a function of the magnitude of the flood at the river mouth. (1) low magnitude flood. The maximum discharge is less than the critical discharge to produce hyperpycnal flows. Failure-induced turbidity currents are generated. (2) Low magnitude flood. The maximum discharge is more than the critical discharge to produce hyperpycnal flows. Hyperpycnal flow forms. A complete sequence with a transitional boundary between inversely graded unit Ha and normally graded unit Hb is deposited. (3) Mid-magnitude sequence. Identical to B but grain size can be coarser and sequence thicker. Sharp contact between Ha and Hb. (4) High-magnitude flood. Same as C but particle deposited are coarser. Erosional surface exists between Ha and Hb. Ha may have been completely eroded during peak flood conditions. Cl, clay; fs, fine silt; ms, medium silt, cs, coarse silt; fsa, fine sand; msa, medium sand (from Mulder et al., 2001a).

doublets. These intrasequence erosional contacts had been produced by laboratory experiments simulating a continuous flow (Duringer, Paicheler, & Schneider, 1991). These authors show facies in ancient deposits that could be interpreted as hyperpycnites, with arenite–siltite alternations or lenses, laminated fine-grained sequences and numerous intrasequence erosional contacts. Similar beds have been recognized in the Var and Zaire turbidite systems (Fig. 10a and b) and in ancient environments (Mavilla, 2000; Mutti et al., 1996, 2000, 2002 and this volume; Fig. 10c). In the case of a low-magnitude flood but with a sufficient discharge to create a hyperpycnal flow (curve 2 in Fig. 9), the transition between Ha and Hb is gradational. In this case, the hyperpycnite can be mistaken with contourite beds defined by Gonthier, Faugères, and Stow (1984), particularly if bioturbation is intense.

If the particle concentration–discharge curve shows no plateau, both flow energy and competency increase slowly, pass through a peak and then decrease slowly. There is no change in the sedimentary structures deposited before, during and after peak flood conditions. However, as the complete Bouma sequence is an exception, the complete hyperpycnite sequence also suffers many exceptions and base truncated hyperpycnite sequences might be more common than the complete sequence.

During higher magnitude flood conditions (curve 3 in Fig. 9), the discharge and velocity reached during the flood peak can be high enough to prevent deposition.

Deposition occurs only when the velocities drop during the period of fall of discharge, and the change in grain-size trend is associated with a sharp contact. During peak conditions of a high-magnitude flood, the Ha unit can be completely eroded and the contact between Ha and Hb is erosive (curve 4 in Fig. 9). This erosion during peak flood conditions generates an intrasequence erosional contact. In this case, there is a shape convergence between the base-truncated hyperpycnite and a classical Bouma-like turbidite sequence deposited by a turbulent surge. Examples of hyperpycnal sequences in ancient environments provided by Mutti et al. (2002) and Mutti et al. (this volume) suggest that preservation of the unit deposited by the waxing flow is rare. A complete discussion of diagnostic features to differentiate hyperpycnite, contourites and classical turbidites is made in Mulder at al. (2002) and summarized in Table 7.

Deposition of hyperpycnites at the mouth of rivers that generate high-frequency turbidity currents can lead to local high sedimentation rates. Mulder, Migeon, Savoye, and Jouanneau (2001b) showed that a core located on a terrace at the mouth of the Var canyon, at 1970 m water depth had sedimentation rates of 1.2–1.6 m per century, for the last

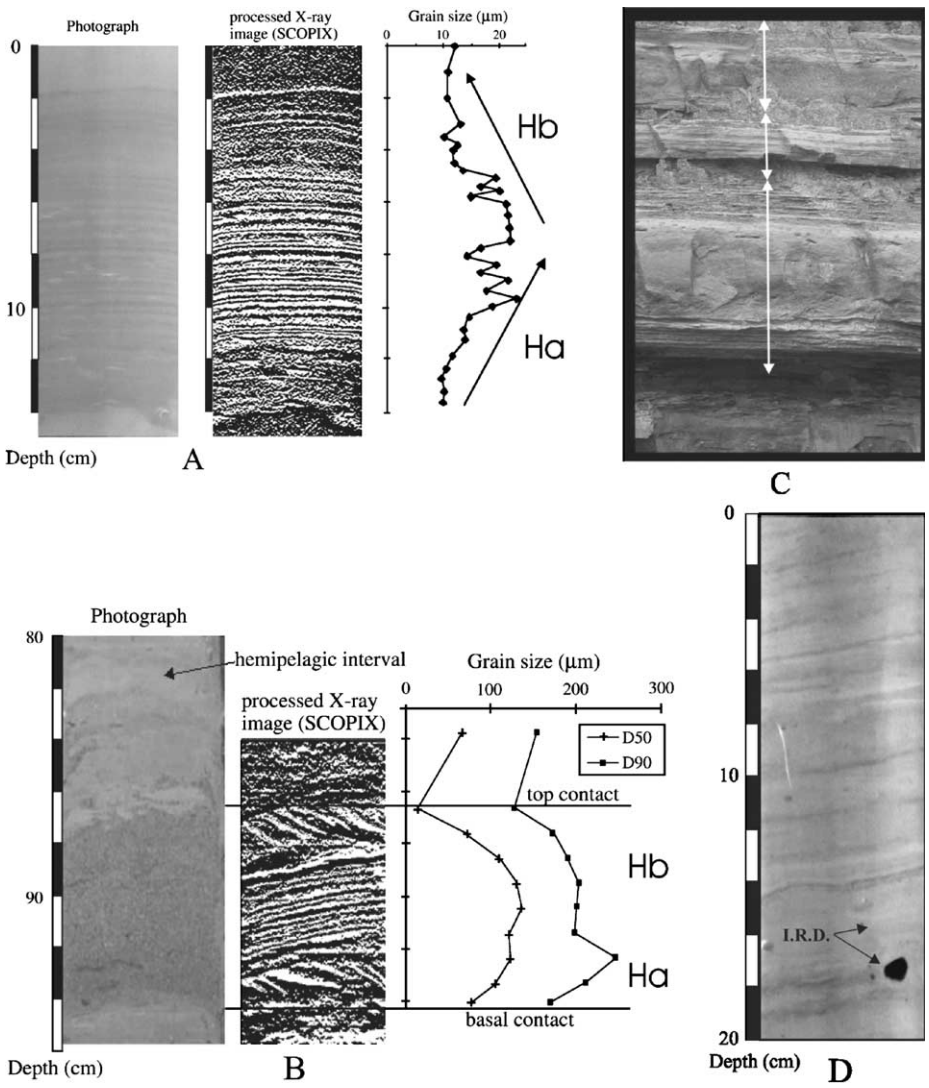

Fig. 10. Complete hyperpycnal turbidite sequence in the Var (A) and Zaire (B) turbidite systems. Note the superposition of the coarsening-up unit, Ha, and the fining-up unit, Hb). (C) Ancient hyperpycnite in the Oligocene Tertiary Piemont Basin, Southern Apennines, Italy (Photograph courtesy of Nicola Mavilla). Arrows indicate extension of single hyperpycnite sequences (D). Fine laminated sequence related to ice melting at the end of the last ice age. I.R.D., ice-rafted detritus.

100 and 50 years, respectively. Thirteen to fourteen hyperpycnites were recorded during the last 100 years and 9–10 were recorded during the 50 last years, which represents a frequency of one hyperpycnal flow every 5–7.5 years. This is consistent with the statistical prediction (Mulder et al., 1997c, 1998a). In the northwestern Bay of Biscay, Zaragosi et al. (2001) described laminated clay and silty clay layers, intensely laminated and containing species of an estuarine dinocyst and a fresh water alga (Fig. 10d). This occurrence dated 15–14.4 BP indicates an increase in European river discharge probably related to melting of the British ice sheet and Alpine glaciers. This suggests that global ice melting could be related to ice-melt intervals. The melting of the Laurentide ice and European ice sheets at the end of the last ice-age could have produced extended major hyperpycnal deposits such those observed in the NAMOC area (North Atlantic; Hesse & Khodabakhsh, 1998; Hesse et al., 1996). These sequences would be associated with the period of increased sedimentation of ice-rafted debris (Heirich events).

Hyperpycnites show that:

- turbidites (i.e. deposits resulting from turbidity currents) can generate coarsening-up facies;
- a waxing flow can form sedimentary structures (Migeon et al., 2001; Mulder et al., 2001a, 2002).
- the presence of erosional or sharp contacts cannot be used anymore as a criteria to define sequence boundaries because high-magnitude floods form such contacts during peak-flood conditions and the bases of laminae might also show erosion. This can lead to a complete re-interpretation of fine-grained series deposited in a river-fed environment such as the beds described by Piper and Deptuck (1997) in the Amazon fan.

Table 7
Recognition criteria of contourite, turbidite (surge deposits) and hyperpycnite (from Mulder et al., 2002)

Bed type	Turbidite sequence (Bouma-like)	Hyperpycnal turbidite sequence (hyperpycnite)	Contourite sequence
Flow type	Turbulent surge	Turbidity current	Contour current
Flow behavior	Unsteady. Mainly waning	Mainly steady. Waxing then waning	Almost completely steady. Waxing then waning
Dominant flow regime	Turbulent	Turbulent	Turbulent
Flow duration and time for deposition	Minutes to days	Hours to weeks	Episodic within 1000s of years
Base contact	Erosive to sharp	Gradational	Gradational
Top contact	Gradational	Gradational	Gradational
Intrabed contact	Infrequent between facies	Erosive to sharp	None
Grading	Clear, normal	Clear, inverse then normal	Crude, inverse then normal
Bioturbation	Absent to intense	Absent to intense	Thorough and intense
Ichnofacies	Few	Few	Many
Structures	Well developed parallel and cross bedding, convolutes	Well developed parallel and cross bedding. Climbing frequent	Crude and sparse parallel and cross bedding. Frequent mottles and lenses
Fauna/flora	Allochtonous mainly marine	Allochtonous mainly continental. Frequent plant and wood fragment	Mainly autochthonous

These new turbidite beds are of major conceptual importance because they bring evidence against several dogmas and paradigms that are related to the initial discovery of turbidites (Bouma, 1962; Kuenen, 1952, 1953).

6.2. Particular hyperpycnites

The draining or breaking of natural and artificial dams and jökulhaups, also form particular hyperpycnites that strongly mimic Bouma-like turbidite sequences.

During these catastrophic extreme events, the river discharge does not follow a classical hydrograph with rising and falling limbs. The hydrograph shows an instantaneous increase in discharge. Discharge values reach quickly a peak and then decrease exponentially. This corresponds to laboratory simulations of surges (Alexander & Mulder, 2003; Garcia, 1994; Garcia & Parker, 1989; Laval, Cremer, Beghin, & Ravenne, 1988; Ravenne & Beghin, 1983). In this case, the hydrodynamic behavior of the flow is highly unsteady, as it is for a slide-induced turbulent surge. However, there are two major differences between the behavior of 'dam-break hyperpycnal flow' and slide-induced turbulent surges. (1) In a 'dam-break flow', the interstitial fluid is initially fresh water. At the continent–ocean boundary or at the aerial–lacustrine interface, a concentration threshold is necessary to generate plunging. It is a hyperpycnal process. (2) The particle concentration might be higher in dam-break hyperpycnal flow than in flood-related hyperpycnal flow, but the flow density never reaches values as high as in the case of slide-induced turbidity currents. For these reasons, we propose to name as 'dam-break hyperpycnal surges' the flows resulting of breaking of dams, including jökulhaups. In the case in which the failure of the dam is due to a flood, the flow can be sustained a long time before and after the passage of the surge. A classical hyperpycnal flow will precede and follow the surge.

Particular hyperpycnites formed by the draining or breaking of dams or jökulhaups are hypothesized in Fig. 11. During an artificial dam break or a jökulhaup (Fig. 11a), a mass flow (hyperconcentrated, concentrated or debris flow) can form simultaneously with an unsteady, turbulent hyperpycnal surge. Deposits will show a fining-up sequence with a basal contact showing intense erosion (Fig. 11a). As the mass flow moves slower than the turbulent surge (Mohrig et al., 1998), a mass flow deposit can be superposed or intercalated with a classical Bouma-like sequence. Both sequences are almost synchronous.

In the case of a natural dam break occurring during a flood, at least two sequences will be superposed. The basal sequence will be a classical mass flow deposit or a Bouma-like turbidite. This sequence is contemporaneous with the river damming. It is directly related to the slide event than dammed the river or to one of the multiple earthquake-induced failures if the damming is due to an earthquake. The top sequence (Fig. 11b) is related to the breaking of the dam. It is identical to the sequence formed by a jökulhaup, i.e. a top cut-out hyperpycnite indicating the beginning of the flood capped with either a mass flow or a hyperconcentrated flow deposit. The end of the flood can be recorded as a base cut-out hyperpycnite. The whole series is close to beds described by Mutti et al. (2002 and this volume) in the Marnoso-arenacea Formation.

In the case of dam erosion during a flood, again several sequences will be superposed (Fig. 11c) but they are not deposited simultaneously. The basal sequence will be a mass flow deposit or a Bouma-like sequence related to a slide triggered simultaneously to the damming. The top sequence is the real sequence of dam draining. It will be a classical hyperpycnite with both the coarsening and

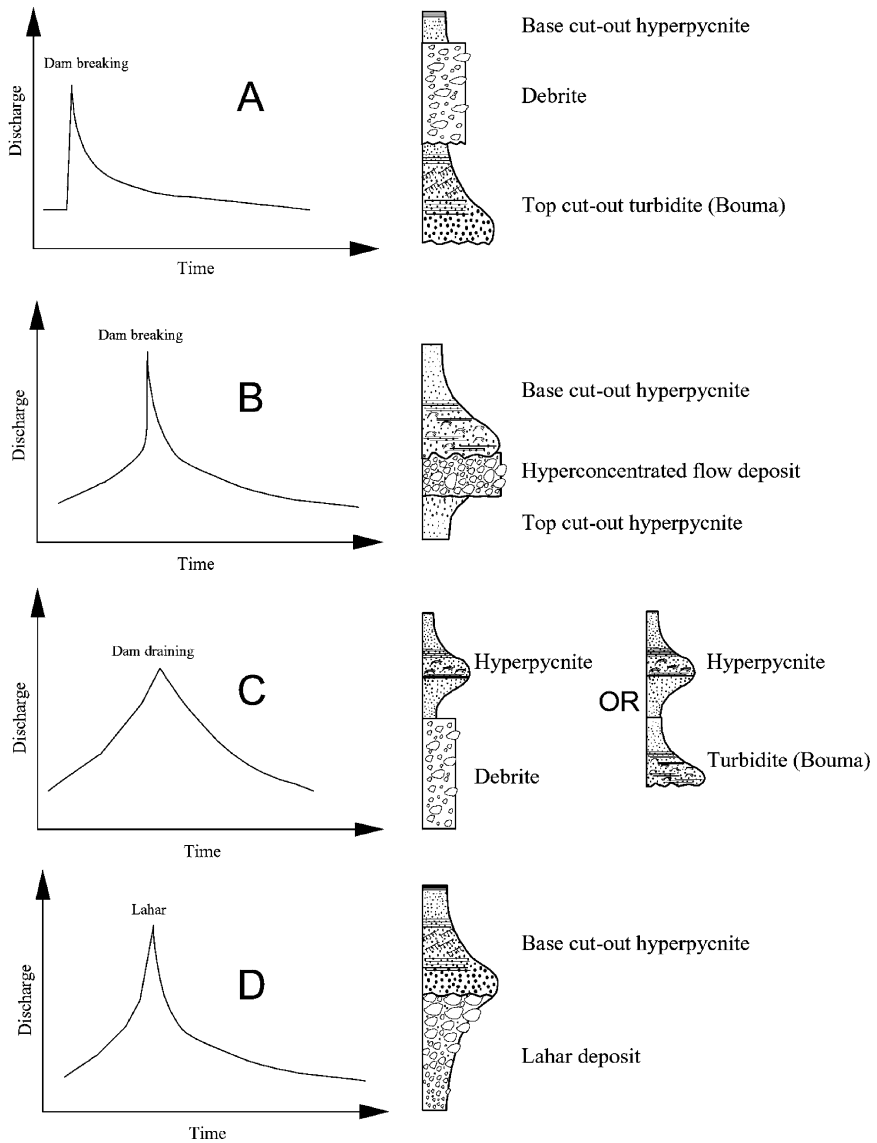

Fig. 11. Flood hydrographs and sedimentary sequences for hyperpycnal turbulent surges. (A) Artificial dam break or a jökulhaups: the hydrograph shows an instantaneous peak and then discharge decreases rapidly. (A) fining-up sequence followed by a mass flow deposit. (B) Natural dam break: the flood hydrograph shows a peak intercalated in an increasing discharge period. Two sequences are stacked. The basal sequence (not represented) is a mass flow deposit contemporaneous of the damming. The top sequence is due to the dam breaking and shows the same sequences as in (A). (C) Erosion of a natural dam. Two sequences are stacked. The basal sequence is a mass flow deposit contemporaneous of the damming. The top sequence is a classical hyperpycnite (1663 AD Saguenay example). (D) Hyperpycnal flow resulting from transformation of a lahar. A complete or truncated hyperpycnite caps a lahar deposit.

fining-up units. In this case, the top sequence will be well developed because the presence of a large amount of easily-erodible material generates a high particle load as happened in 1663 AD in the Saguenay.

Lahars are triggered by heavy rainfalls. Lahars-related hyperpycnites (Fig. 11d) show a lahar deposit intercalated with a hyperpycnite. As it is related to sudden erosion of soft material, and high energy flow, the base of the hyperpycnite might be not deposited or eroded.

In these examples of particular hyperpycnites, the sedimentary record show stacked beds indicating several processes that are either simultaneous or separated by a short period of time. Such associations have been observed in lakes (Linier, 2001) and in the Saguenay Fjord (Saint-Onge et al., in press).

6.3. Changes in hyperpycnite deposition with relative sea-level changes

Evolution of activity of hyperpycnal flows with relative sea-level changes and/or climatic changes should be important as hyperpycnal flows are mainly related to flood magnitude and frequency. As discharge and particle load are controlled by climate (latitude, mean temperature) and drainage basin morphology (surface and altitude), we can estimate the evolution of hyperpycnal flow activity

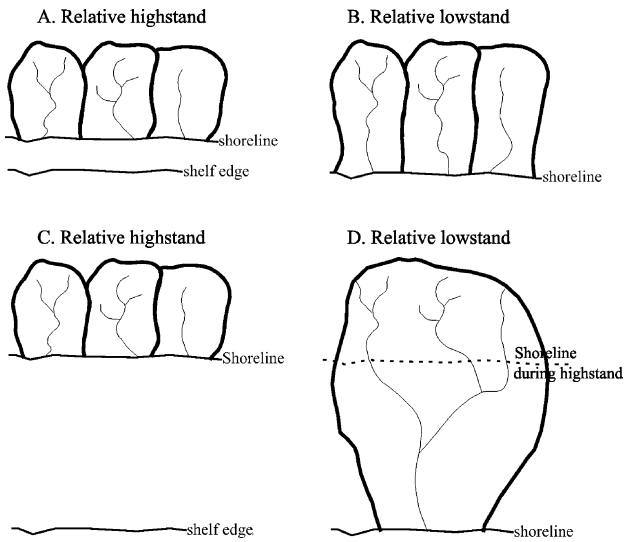

Fig. 12. Hyperpycnal activity and relative sea-level changes. (A) Relative sea-level highstand and narrow continental shelf. (B) Relative sea-level lowstand and narrow continental shelf. Increase in hyperpycnal activity because rivers discharge at the shelfbreak. (C) Relative sea-level highstand and large continental shelf. (D) Relative sea-level lowstand and large continental shelf. Decrease in hyperpycnal activity because river merging tend to form giant rivers. Bold lines represent limits of drainage basins. See text for comments.

as follows: Hyperpycnal activity (frequency and magnitude) will increase if:

- climate becomes more arid (colder or warmer): reduction of vegetal cover and increase of temperature variations will intensify erosion and so will suspended particle concentration,
- relative sea level falls in an area with a reduced continental shelf. Rivers discharge directly in canyon heads,
- relative sea level rises in an area with a large continental shelf. Giant basins tend to split into small basins with a higher potential for hyperpycnal flow formation (Fig. 12).

Conversely, hyperpycnal activity will decrease if:

- climate becomes wetter: intensification of vegetal cover will protect emerged lands from erosion and particle load will be more dilute,
- relative sea level falls in an area with a large continental shelf. Rivers will tend to merge and to form giant rivers that produce less hyperpycnal flows than small rivers (Mulder & Syvitski, 1996). This is what happened on the shelf located between France and England during the last lowstand. Rivers such as Rhine, Seine, Meuse and Thames merged to form a giant 'Channel River' (Mulder & Syvitski, 1996; Fig. 12),
- relative sea level rises in an area with a small continental shelf. River mouths disconnect from canyon heads,
- the emerged land is partially or fully covered with ice. River activity becomes temporary or even stops. Only sporadic hyperpycnal turbulent surges will form, either due to the breaking of morainic dams or to local ice melting during volcanic eruptions on active margins.

Areas with high tectonic activity tend to develop small basins connected to small drainage basins with high relief. Rivers flowing in such environments are good candidates to form hyperpycnal flows (Mutti et al., 1996, 2000).

7. Role of hyperpycnal flows in canyon formation and channel meandering

Canyons are incised valleys with steep sides and a steep mean slope between canyon head and mouth (Shepard & Dill, 1966). Canyon head and sides usually show failure scars. Several hypothesis are usually given for their formation.

The subaerial hypothesis.

Canyons would form by river erosion or erosion under shallow water during relative sea-level lowstands. This erosion would be important because of a drastic fall of the base level. This hypothesis is realistic for Mediterranean canyons that began to grow after the Messinian crisis (Clauzon, 1978; Clauzon, Rubino, & Savoye, 1995; Savoye & Piper, 1991; Savoye, Piper, & Droz, 1993). For other canyons in the world, this would suggest a canyon origin during the early phases of rifting and ocean opening, i.e. the Cretaceous for North Atlantic and the Jurassic for the South Atlantic.

The submarine hypothesis.

A first hypothesis suggests that canyon incision would form by retrogressive erosion (Guillocheau, Pautot, & Auzende, 1982). The canyon head would move landward, which is consistent with the numerous slumps scars that are observed at this location. Other evidence supporting this hypothesis is the frequency of pockmarks aligned in the direction of the canyons, beyond the head in the landward direction (Cirac, personal communication; Le Moigne, 1999). These pockmarks suggest fluid upward motion and deep disorganization of sedimentary series. These pockmarks could either result from the sediment disorganization in the direction of retrogression, or indicate weakness lineaments that direct retrogression. This would be consistent with the fact that canyons follow regional tectonic directions (Cirac et al., 2001).

A second hypothesis suggests that canyons could be 'constructed structures'. In fact, they would be 'by pass' areas in a globally prograding margins. They would represent the narrow areas where margins do not prograde (Faugères, Stow, Imbert, & Viana, 1999; Pratson & Haxby, 1996).

The third hypothesis suggests that canyons would result from intense erosion by downslope eroding sediment flows (Pratson, Ryan, Mountain, & Twitchell, 1994). This hypothesis has arisen when in situ measurements have

revealed a sporadic or continuous activity of particle-laden flows in canyons (Gennesseaux et al., 1971; Hay, 1987; Inman, 1970; Shepard & Dill, 1966; Shepard, Marshall, McLoughlin, & Sullivan, 1979; Shepard, McLoughlin, Marshall, & Sullivan, 1977; Weirich, 1984). Because major canyons are usually connected to a river (Amazon; Hiscott et al., 1997; Zaire; Droz, Rigaut, Cochonat, & Tofani, 1996; Savoye et al., 2000), the canyon head is located in an area where sediment accumulation rates are important. The importance of erosion suggests that canyons are formed by either very frequent slide-induced turbulent surges or by long-duration hyperpycnal flows.

The recent discovery of a turbidite deposited in 1999 in the Capbreton canyon (Mulder, Weber, Anschutz, Jorissen, & Jouanneau, 2001c) or hyperpycnal activity in the Var canyon tends to support this hypothesis. At least, this important turbidity current activity during the present relative highstand of sea-level suggests that the freshness of the present submarine canyon located seaward of a river mouth is due to sporadic turbidity current activity, and that hyperpycnal processes represents a substantial part of this activity.

Another evidence supporting the role of hyperpycnal flows in construction of deep-sea turbidite systems connected to a river is the frequent meandering shape of channels in channel–levee complexes. Channels tend to have high sinuosity defined as the measurement of the trend of a flow to move in a straightforward direction. Meanders can be due to the resistance of any flow at its basal interface (Gorycki, 1973). This would explain that meanders are ubiquitous features of channels in various environments. Meandering depends on hydrodynamic and morphologic thresholds. A channel remains straight for low slopes. Above a slope threshold, meanders form (Schumm & Khan, 1972).

Conversely, an increase in discharge that can be related to an increase in slope, tends to increase sinuosity but also decreases the slope threshold to generate meander formation. As a consequence, meanders will appear for high-discharge flow moving on low slopes or lower discharge flows moving along slightly steeper slopes. These observations suggest that meanders would occur on moderate to low slopes by high-energy, low-concentrated flows maintained over long periods (Leopold & Maddock, 1953; Rigaut, 1997; Schumm, 1981; Schumm & Kahn, 1972). Hyperpycnal flows are excellent candidates to explain the origin of meandering in deep channels and submarine canyons.

There are many other currents that are not related to sediment transport that could erode canyons. In the polar regions where sea ice forms, associated brine rejection cause density currents to flow across continental shelves and accelerate down the slope. These currents flow at velocities great enough to erode the seafloor. They occur annually and may last for weeks to months (O'Grady & Syvitski, 2003). Similar lasting currents form during cooling episodes along many margins. For example density currents that are cooled during the Mediterranean winter flow at high velocities down the floor of the Adriatic, and also across the Gulf of Lions and down canyons each year (Canals, personal communication, 2002).

Finally tidally generated currents and the breaking of internal waves offer still other mechanisms to erode the continental slope and contribute to the formation and maintenance of canyons.

8. Conclusions and perspective

Marine hyperpycnal flows form when fresh water effluent discharges into the ocean with a suspended mater content of 36–43 kg m^{-3}. These limits can be substantially decreased by convective instability and local hydrodynamic or climatic conditions. Hyperpycnal turbulent surges can also form when an artificial or a natural dam breaks or drains. They may form due to the action of jökulhaups or lahars. This suggests that probably most of the world rivers can generate sporadic to frequent hyperpycnal flows.

Hyperpycnal flows are frequent in lakes where only small particle concentrations are necessary for plunging. They have been monitored at sea at the mouth the Huanghe (China), one of world's dirtiest rivers. They can last hours to month. Because they are triggered during large or extreme floods, they can bring a considerable volume of particles towards the sea. They might represent a large proportion of fine-grained turbidite deposited in river-fed turbidite systems. A major difference between hyperpycnal processes and classical slide-induced turbidity currents, is that the initial internal fluid of hyperpycnal flows is fresh water. This strongly reduces the difference between flow and ambient water densities and explains why hyperpycnal flows are slow-moving and turbulent ignitive surges are initially fast-moving flows. In addition, hyperpycnality has to be maintained despite particle deposition. This is achieved by entrainment and mixing of salt water with the ambient fluid. As they are usually long-duration phenomena, hyperpycnal flows can affect the biology and chemistry of environments in which they form, particularly when in restricted environments such as fjords, inlets, canyons or pounded basins.

Deposits related to flood-generated turbidity currents have been discovered in recent deposits of the Saguenay Fjord, the Var and Zaire deep-sea fans. High sedimentation rates observed on margins that once received ice-melt during the last glacial period could be due to numerous hyperpycnite stacking that deposited during periods of ice melting. In the Oligocene series of the Apennines, small river-fed basins in tectonically active environments show also evidence of hyperpycnites. The two-unit sequence that forms a complete hyperpycnite is related to the evolution of the flood hydrograph. The basal coarsening-up unit is deposited by the waxing flow generated during

the increasing discharge period and the top fining-up unit is deposited by the waning flow generated during the decreasing discharge period. These sequences can be base-truncated due to erosion by high-velocity flows developed during peak condition of high-magnitude floods. Intrabed contacts can be frequent. Hyperpycnal surges deposit sequence couplets. The mass-flow deposit caps or is intercalated in a fining-up sequence with heavy erosion at is basal contact. Hyperpycnal deposition can generate sedimentation rates that are locally larger than $10\ m\ ky^{-1}$. Hyperpycnal processes could also play an important role in canyon formation and in the origin of meanders in deep-sea channels. Because they are related to climate through flood frequency and magnitude, they are subject to variations during climatic and eustatic variations. The way they vary, increase or decrease in their frequency and magnitude, depends of the climatic changes (wetter or dryer) and the morphology of the continental shelf at a river mouth. This characteristic suggests that hyperpycnites are good tools to decipher climatic archives in sedimentary rocks deposited un a deep marine environment.

Acknowledgements

Jan Alexander, Jasim Imran, Nicola Mavilla, Emiliano Mutti, Gary Parker, Jeff Parsons, David Piper, Lincoln Pratson, Jean-Jacques Tiercelin, Guillaume Saint-Onge, and Sébastien Zaragosi are thanked for their insights and advances that we have incorporated into our review paper. Brad Prather and Gary Scott Steffens are thanked for the substantial review of the paper. UMR CNRS 5805 EPOC Contribution number 1461.

References

Akiyama, J., & Stefan, H. G. (1984). Plunging flow into a reservoir—theory. *Journal of Hydraulic Engineering*, *110*, 484–499.

Akiyama, J., & Stefan, H. G. (1988). Turbidity-current simulation in a diverging channel. *Water Resources Research*, *24*, 579–587.

Alexander, J., & Morris, S. (1994). Observations on experimental, nonchannelized, high-concentration turbidity currents and variations in deposits around obstacles. *Journal of Sedimentary Research*, *A64*, 899–909.

Alexander, J., & Mulder, T. (2002). Experimental quasi-steady density current.. *Marine Geology*, *186*, 195–210.

Arnaud, F., Linier, V., Desmet, M., Revel, M., Beck, C., Paterne, M., Pourchet, M., & Tribovillard, N. (2001). *Carottage long d'un lac d'altitude (Lac d'Anterne, Haute Savoie): implications paléoclimatiques et paléosismiques. 8ème Congress of ASF, Orléans, France, Book of Abstracts, ASF Publ. 36*, p. 17.

Bagnold, R. A. (1962). Auto-suspension of transported sediment; turbidity currents. *Royal Society (London), Proceedings, Series A*, *265*, 315–319.

Bates, C. C. (1953). Rational theory of delta formation. *Bulletin of American Association of Petroleum Geology*, *37*(9), 2119–2162.

Bellier, J. (1967). *Le barrage de Malpasset, travaux*, 363–383.

Bornhold, B. D., Ren, P., & Prior, D. B. (1994). High-frequency turbidity currents in British Columbia fjords. *Geo-Marine Letters*, *14*, 238–243.

Bouma, A. H. (1962). *Sedimentology of some Flysch deposits. A graphic approach to facies interpretation*. Amsterdam: Elsevier, 168p.

Bourcart, J. (1964). Les sables profonds de la Méditerranée occidentale. In A. H. Bouma, & A. Brouwer (Eds.), *Developments in sedimentology no. 3, turbidites* (pp. 148–155). Amsterdam: Elsevier.

Bournet, P. E., Dartus, D., Tassin, B., & Vincon-Leite, B. (1999). Numerical investigation of plunging density current. *Journal of Hydraulic Engineering*, *125*(6), 584–594.

Brown, W. M., & Ritter, J. M. (1971). *Sediment transport and turbidity in the Eel River Basin, California. US Geological Survey Water-Supply Paper, 1986*.

Chikita, K. (1991). Dynamic processes of sedimentation by river induced turbidity currents. II. Application of a two-dimensional, advective diffusion model. *Japan Geomorphological Union, Transactions*, *13-1*, 1–18.

Cirac, P., Bourillet, J.-F., Griboulard, R., Normand, A., Mulder, T., & the ITSAS shipboard scientific party, (2001). Le canyon de Capbreton: nouvelles approches morphostructurales et morphosédimentaires. Premiers résultats de la campagne Itsas. *Comptes Rendus de l'Academie des Sciences, Paris*, *332*, 447–455.

Clauzon, G. (1978). The Messinian Var Canyon (Provence, southern France). Paleogeographic implications. *Marine Geology*, *27*(3/4), 231–246.

Clauzon, G., Rubino, J.-L., & Savoye, B. (1995). *Marine Pliocene Gilbert-type fan deltas along the French Mediterranean coast. In: IAS-16th regional meeting of sedimentology—5ème congrès français de sédimentologie—ASF. Field-trip guide book, 23*, Paris: Publications ASF, pp. 143–222.

Droz, L., Rigaut, F., Cochonat, P., & Tofani, R. (1996). Morphology and recent evolution of the Zaire turbidite system (Gulf of Guinea). *Geological Society of American Bulletin*, *108*, 253–269.

Duringer, P., Paicheler, J.-C., & Schneider, J.-L. (1991). Un courant d'eau peut-il générer des turbidites? Résultats d'expérimentations analogiques. *Marine Geology*, *99*, 231–246.

Einarsson, P., Brandsdóttir, B., Tumi Gudmunsson, M., Björnsson, H., Grönvold, K., & Sigmundsson, F. (1997). Center of the Iceland Hotspot Experiences Volcanic Unrest. *Eos Transactions, American Geophysical Union*, *78*(35), 369–375.

Emmett, W. W. (1982). Measurements of bedloads in rivers: erosion and particle transport measurements. *International Association for Hydrological Science Publication*, *122*, 3–13.

Emms, P. W. (1999). On the ignition of geostrophically rotating turbidity currents. *Sedimentology*, *46*, 1049–1063.

Farrell, G., & Stefan, H. G. (1989). Mathematical modeling of plunging reservoir flows. *Journal of Hydraulic Research*, *26*, 525–537.

Faugères, J.-C., Stow, D. A. V., Imbert, P., & Viana, A. (1999). Seismic feature diagnostic of contourite drifts. *Marine Geology*, *162*, 1–38.

Forel, F. A. (1885). Les ravins sous-lacustres des fleuves glaciaires. *Comptes Rendus de l'Academie des Sciences, Paris*, *101*(16), 725–728.

Forel, F. A. (1892). *Le Léman: Monographie Limnologique 1*. Lausanne: F. Rouge, 543p.

Friedrichs, C. T., Wright, L. D., Hepworth, D. A., & Kim, S. C. (2000). Bottom-boundary-layer processes associated with fine sediment accumulation in coastal seas and bays. *Continental Shelf Research*, *20*, 807–841.

Fukushima, Y., Parker, G., & Pantin, H. M. (1985). Prediction of ignitive turbidity currents in Scripps submarine canyon. *Marine Geology*, *67*, 55–81.

Garcia, M. H. (1994). Depositional turbidity currents laden with poorly sorted sediment. *Journal of Hydraulic Engineering*, *120*, 1240–1263.

Garcia, M. H., & Parker, G. (1984). *On the numerical prediction of turbidity currents* (pp. 1556–1565). *Third International Symposium on River Sedimentation*, Mississippi: The University of Mississippi.

Garcia, M. H., & Parker, G. (1989). Experiments on hydraulic jumps in turbidity currents near a canyon-fan transition. *Science*, *245*, 393–396.

Garcia, M. H., & Parker, G. (1993). Experiments on the entrainment of sediment into suspension by a dense bottom current. *Journal of Geophysical Research*, *98*(3), 4793–4807.

Gennesseaux, M., Guibout, M., & Lacombe, H. (1971). Enregistrement de courants de turbidité dans la vallée sous-marine du Var (Alpes-Maritimes). *Comptes Rendus de l'Academie des Sciences, Paris, Série D*, *273*, 2456–2459.

Gennesseaux, M., Mauffret, A., & Pautot, G. (1980). Les glissements sous-marins de la pente continentale niçoise et la rupture de câbles en mer Ligure (Méditerranée Occidentale). *Comptes Rendus de l'Academie des Sciences, Paris*, *290*, 959–962.

Gonthier, E., Faugères, J.-C., & Stow, D. A. V. (1984). Contourite facies of the Faro drift, Gulf of Cadiz. In D. A. V. Stow, & D. J. W. Piper (Eds.), *Fine-grained sediments: deep water processes and facies* (pp. 245–256). *Geological Society of London, Special Publication, 15*.

Gorsline, D. S., de Diego, T., & Nava-Sanchez, E. H. (2000). Seismically triggered turbidites in small margin basins: Alfonso Basin, Western Gulf of California and Santa Monica Basin, California Borderland. *Sedimentary Geology*, *135*, 21–35.

Gorycki, M. A. (1973). Hydraulic drag: a meander initiating mechanism. *Geological Society of American Bulletin*, *84*, 175–186.

Gould, H. R. (1951). *Some quantitative aspects of Lake Mead turbidity currents*. *Society of Economic Paleontologists and Mineralogists Special Publication, 2*, pp. 34–52.

Grönvold, K., & Jóhannesson, H. (1984). Eruption in Grímsvötn 1983, course of events and chemical studies of the tephra. *Jökul*, *34*, 1–11.

Gudmunsson, M. T., Sigmundsson, F., & Björnsson, H. (1997). Ice–volcano interaction of the 1996 Gjálp subglacial eruption, Vatnajökull, Iceland. *Nature*, *389*, 954–957.

Guillocheau, F., Pautot, G., & Auzende, J.-M. (1982). Les canyons du Var et du Paillon (marge des Alpes méridionales-Méditerranée occidentale): une origine quaternaire par glissement. *Comptes Rendus de l'Academie des Sciences, Paris*, *296*, 91–96.

Hack, J. T. (1957). *Studies of longitudinal stream profiles in Virginia and Maryland. US Geological Survey Professional Paper 294-B*.

Hay, A. E. (1987). Turbidity currents and submarine channel formation in Rupert Inlet, British Columbia. 2. The roles of continuous and surge-type flow. *Journal of Geophysical Research*, *92*, 2883–2900.

Hesse, R., & Chough, S. K. (1980). The Northwest Atlantic Mid-Ocean Channel of the Labrador Sea: II. Deposition of parallel laminated levee-mud from the viscous sublayer of low-density turbidity currents. *Sedimentology*, *27*, 697–711.

Hesse, R., & Khodabakhsh, S. (1998). Depositional facies of late Pleistocene Heinrich events in the Labrador Sea. *Geology*, *26*(2), 103–106.

Hesse, R., Klauke, I., Ryan, W. B. F., Edwards, M. B., Piper, D. J. W., & NAMOC Study Group, (1996). Imaging Laurentide ice sheet drainage into the deep sea: impact on sediments and bottom water. *Geological Society of America Today*, 3–9.

Hiscott, R. N., Pirmez, C., & Flood, R. D. (1997). Amazon submarine fan drilling. A big step forward for deep-sea fan models. *Geoscience Canada*, *24*, 13–24.

Hoyal, D. C., Bursik, M. I., & Atkinson, J. F. (1999). Settling-driven convection: a mechanism of sedimentation from stratified fluids. *Journal of Geophysical Research*, *104*, 7953–7966.

Hughen, K. A., Overpeck, J. T., & Anderson, R. F. (2000). Recent warming in a 500-year paleotemperature record from varved sediments, Upper Soper Lake, Baffin Island, Canada. *The Holocene*, *10-1*, 9–19.

Hughes-Clarke, J. E. (1990). Late stage slope failure in the wake of the 1929 Grand Banks earthquake. *Geo-Marine Letters*, *10*, 69–79.

Hughes-Clarke, J. E., Shor, A. N., Piper, D. J. W., & Mayer, L. A. (1990). Large-scale current-induced erosion and deposition in the path of the 1929 Grand Banks turbidity current. *Sedimentology*, *37*, 613–629.

Imran, J., Parker, G., & Katopodes, N. (1998). A numerical model of channel inception on submarine fans. *Journal of Geophysical Research*, *103*(C1), 1219–1238.

Imran, J., & Syvitski, J. (2000). Impact of extreme river events on coastal oceans. *Oceanography*, *13*(3), 85–92.

Inman, D. L. (1970). Strong currents in submarine canyons. *Abstract of the Transactions, American Geophysical Union*, *51*, 319.

Kassem, A., & Imran, J. (2001). Simulation of turbid underflow generated by the plunging of a river. *Geology*, *29*(7), 655–658.

Kennish, M. J. (1989). *Practical handbook of marine science*. Boca Raton, FL: CRC Press, 710p.

Kneller, B. (1995). Beyond the turbidite paradigm: physical models for deposition of turbidites and their implications for reservoir prediction. In A. J. Hartley, & D. J. Prosser (Eds.), *Characterization of deep marine clastic systems* (pp. 31–49). *Geological Society of London, Special Publication, 94*.

Kneller, B. C., & Branney, M. J. (1995). Sustained high-density turbidity currents and the deposition of thick massive beds. *Sedimentology*, *42*, 607–616.

Kneller, B. C., & Buckee, M. J. (2000). The structure and fluid mechanics of turbidity currents: a review of some recent studies and their geological implications. *Sedimentology*, *47*, 62–94.

Kuenen, P. H. (1952). Estimated size of the Grand Banks turbidity current. *American Journal of Science*, *250*, 849–873.

Kuenen, P. H. (1953). Significant features of graded bedding. *American Association of Petroleum Geologists Bulletin*, *37*, 1044–1066.

Kuenen, P. H., & Migliorini, C. I. (1950). Turbidity currents as a cause of graded bedding. *Journal of Geology*, *58*, 91–127.

Lambert, A. M., Kelts, K. R., & Marshall, N. F. (1976). Measurement of density underflows from Walensee, Switzerland. *Sedimentology*, *23*, 87–105.

Laval, A., Cremer, M., Beghin, P., & Ravenne, C. (1988). Density surges: two-dimensional experiments. *Sedimentology*, *35*, 73–84.

Le Moigne, M. (1999). *Compréhension des mécanismes de formation des pockmarks sur la pente du Golfe de Guinée*. Lille: DEA, University of Science and Technology, 62p.

Leopold, L. B., & Maddock, T., Jr. (1953). *The hydraulic geometry of stream channels and some physiographic implications*. *US Geological Survey Professional Paper 252*, 53p.

Letourneur, J., & Michel, R. (1971). *Géologie du génie civil, Collection U*. Paris: Armand Colin, 728p.

Linier, V., (2001). *Mécanismes et conditions de l'enregistrement de la sismicité dans des sédiments lacustres*. PhD Thesis, Univ. de Savoie

Linier, V., Arnaud, F., Beck, C., Desmet, M., Trentessaux, A., & Pourchet, M. (2001). Discriminating flood deposits from turbiditic reworking of delta foreset, in a terrigenous-fed lake: a clue to separate run off peaks (climatic events) from in situ destabilization (seismo-tectonic events). *Eighth Congress of ASF, Orléans, France. Book of Abstracts, ASF Publ., 36*, 229.

Lowe, D. R. (1979). Sediment gravity flows: their classification and some problems of application to natural flows and deposits. In L. J. Doyle, & O. H. Pilkey (Eds.), *Geology of Continental Slopes* (pp. 75–82). *Society of Economic Paleontologists and Mineralogists Special Publication, 27*.

Lowe, D. R. (1982). Sediment gravity flows: II. Depositional models with special reference to the deposits of high-density turbidity currents. *Journal of Sedimentary Petrology*, *52*, 279–297.

Luthi, S. (1981). Experiments on non-channelized turbidity currents and their deposits. *Marine Geology*, *40*, M59–M68.

Malinverno, A., Ryan, W. B. F., Auffret, G. A., & Pautot, G. (1988). Sonar images of the Path of Recent Failure Events on the Continental Margin off Nice, France. In H. F. Clifton (Ed.), *Sedimentological consequences of convulsive geologic events* (pp. 59–75). *Geological Society of America Special Paper, 229*.

Matthai, H. F. (1990). In M. G. Woolman, & H. C. Riggs (Eds.), *The Geology of North America, Vol. O1, Surface Water Hydrology* (pp. 97–120). Boulder, CO: Geological Society of America.

Mavilla, N., (2000). *Stratigraphie et analyse de faciès de la succession d'âge oligo-miocène du bassin tertiaire piémontais (Italie nord occidentale* (225p). PhD Thesis, Univ. Bordeaux 1

Maxworthy, T. (1999). The dynamics of sedimenting surface gravity currents. *Journal of Fluid Mechanics*, *392*, 27–44.

Mc Cave, I. N. (1986). Local and global aspects of the bottom nepheloid layers in the world ocean. *Netherland Journal of Deep-Sea Research*, *20*(2/3), 167–181.

Meade, R. H. (1996). River-sediment inputs to major deltas. In J. D. Milliman, & B. U. Haq (Eds.), *Sea-level rise and coastal subsidence* (pp. 63–85). Dordrecht: Kluwer.

Middleton, G. V. (1967). Experiments on density and turbidity currents. III. Deposition of sediment. *Canadian Journal of Earth Science*, *4*, 475–505.

Middleton, G. V. (1976). Hydraulic interpretation of sand size distributions. *Journal of Geology*, *84*, 405–426.

Middleton, G. V. (1993). Sediment deposition from turbidity currents. *Annual Review of Earth and Planetary Sciences*, *21*, 89–114.

Middleton, G. V., & Hampton, M. A. (1973). Sediment gravity flows: mechanics of flow and deposition. In G. V. Middleton, & A. H. Bouma (Eds.), *Turbidites and deep-water sedimentation* (pp. 1–38). *Society of Economic Paleontologists and Mineralogists Special Publication*.

Middleton, G. V., & Hampton, M. A. (1976). Subaqueous sediment transport and deposition by sediment gravity flows. In D. J. Stanley, & D. J. P. Swift (Eds.), *Marine sediment transport and environmental management* (pp. 197–218). New York: Wiley.

Migeon, S., (2000). *Dunes géantes et levées sédimentaires en domaine marin profond: approche morphologique, sismique et sédimentologique* (288p). PhD Thesis, Univ. Bordeaux 1

Migeon, S., Savoye, B., Zanella, E., Mulder, T., Faugères, J. C., & Weber, O. (2001). Detailed seismic and sedimentary study of turbidite sediment waves one the Var sedimentary ridge (SE France): significance for sediment transport and deposition and for the mechanism of sediment wave construction. *Marine and Petroleum Geology*, *18*, 179–208.

Migeon, S., Weber, O., Faugères, J.-C., & Saint-Paul, J. (1999). SCOPIX: a new X-ray imaging system for core analysis. *Geo-Marine Letters*, *18*, 251–255.

Milliman, J. D., & Meade, R. H. (1983). World-wide delivery of river sediment to the oceans. *Journal of Geology*, *91*, 1–21.

Milliman, J. D., & Syvitski, J. P. M. (1992). Geomorphic/tectonic control of sediment discharge to the ocean: the importance of small mountainous rivers. *Journal of Geology*, *100*, 525–544.

Mohrig, D., Whipple, K. X., Hondzo, M., Ellis, C., & Parker, G. (1998). Hydroplaning of subaqueous debris flows. *Geological Society of American Bulletin*, *110*, 387–394.

Morehead, M. D., Syvitski, J. P. M., Hutton, E. W. H., & Peckham, S. D. (2003). Modeling the inter-annual and intra-annual variability in the flux of sediment in ungauged river basins. *Global and Planetary Change*, *39*(1/2), 95–110.

Mulder, T., & Alexander, J. (2001). The physical character of subaqueous sedimentary density currents and their deposits. *Sedimentology*, *48*, 269–299.

Mulder, T., & Cochonat, P. (1996). Classification of offshore mass movements. *Journal of Sedimentary Research*, *66*, 43–57.

Mulder, T., Migeon, S., Savoye, B., & Faugères, J.-C. (2001a). Inversely-graded turbidite sequences in the deep Mediterranean. A record of deposits from flood-generated turbidity currents? *Geo-Marine Letters*, *21*, 86–93.

Mulder, T., Migeon, S., Savoye, B., & Faugères, J.-C. (2002). Inversely-graded turbidite sequences in the deep Mediterranean. A record of deposits from flood-generated turbidity currents? A reply. *Geo-Marine Letters*, *22*(2), 112–120.

Mulder, T., Migeon, S., Savoye, B., & Jouanneau, J.-M. (2001b). Twentieth century floods recorded in the deep Mediterranean sediments. *Geology*, (11), 1011–1014.

Mulder, T., Savoye, B., Piper, D. J. W., & Syvitski, J. P. M. (1998a). The Var submarine sedimentary system: understanding Holocene sediment delivery processes and their importance to the geological record. In M. S. Stocker, D. Evans, & A. Cramp (Eds.), *Geological processes on continental margins: sedimentation, mass-wasting and stability* (pp. 145–166). *Geological Society of London, Special Publication 129*.

Mulder, T., Savoye, B., & Syvitski, J. P. M. (1997a). Numerical modelling of a mid-sized gravity flow: the 1979 Nice turbidity current (dynamics, processes, sediment budget and seafloor impact). *Sedimentology*, *44*, 305–326.

Mulder, T., Savoye, B., Syvitski, J. P. M., & Cochonat, P. (1997b). Origine des courants de turbidité enregistrés à l'embouchure du Var en 1971. *Comptes Rendus de l'Academie des Sciences, Paris, Serie IIa*, *322*(4), 301–307.

Mulder, T., Savoye, B., Syvitski, J. P. M., & Parize, O. (1997c). Des courants de turbidité hyperpycnaux dans la tête du canyon du Var? Données hydrologiques et observations de terrain. *Oceanologica Acta*, *20*, 607–626.

Mulder, T., & Syvitski, J. P. M. (1995). Turbidity currents generated at river mouths during exceptional discharges to the world oceans. *Journal of Geology*, *103*, 285–299.

Mulder, T., & Syvitski, J. P. M. (1996). Climatic and morphologic relationships of rivers: implications of sea level fluctuations on river loads. *Journal of Geology*, *104*, 509–523.

Mulder, T., Syvitski, J. P. M., & Skene, K. I. (1998b). Modelling of erosion and deposition by turbidity currents generated at river mouths. *Journal of Sedimentary Research*, *68*, 124–137.

Mulder, T., Weber, O., Anschutz, P., Jorissen, F. J., & Jouanneau, J.-M. (2001c). A few months-old storm-generated turbidite deposited in the Capbreton Canyon (Bay of Biscay, S-W France). *Geo-Marine Letters*, *21*(3), 149–156.

Mullenbach, B. L., & Nittrouer, C. A. (2000). Rapid deposition of fluvial sediment in the Eel canyon, northern California. *Continental Shelf Research*, *20*, 2191–2212.

Mutti, E., Davoli, G., Tinterri, R., & Zavala, C. (1996). The importance of ancient fluvio-deltaic systems dominated by catastrophic flooding in tectonnically active basins. *Memorie di Scienze Geologiche*, *48*, 233–291.

Mutti, E., Ricci Lucchi, F., & Roveri, M. (2002). *Revisiting turbidites of the Marnoso-arenacea formation and their basin-margin equivalents: problems with classic models. Excursion guidebook of the turbidite workshop, Parma, Italy, 21–22 May 2002*.

Mutti, E., Tinterri, R., Benevelli, G., Angella, S., di Biase, D., Cavanna, G., (2003). Deltaic, mixed and turbidite sedimentation of ancient foreland basins, Marine and Petroleum Geology, this issue (doi:10.1016/j.marpetgeo. 2003.09.001).

Mutti, E., Tinterri, R., di Biase, D., Fava, L., Mavilla, N., Angella, S., & Calabrese, L. (2000). Delta-front facies associations on ancient flood-dominated fluvio-deltaic systems. *Reviews of the Society of Geology Espana*, *13*(2), 165–190.

Nardin, T. R., Hein, F. J., Gorsline, D. S., & Edwards, B. D. (1979). A review of mass movement processes and acoustic characteristics, and contrasts in slope and base-of-slope systems versus canyon-fan-basin floor systems. In L. J. Doyle, & O. H. Pilkey (Eds.), *Geology of continental slopes* (pp. 61–73). *Society of Economic Paleontologists and Mineralogists Special Publication, 27*.

Nava-Sanchez, E. H., Gorsline, D. S., Cruz-Orozco, R., & Godinez-Orta, L. (1999). The El Coyote fan delta: a wave-dominated example from the Gulf of California, Mexico. *Quaternary International*, *56*, 129–140.

Nelson, C. H., Karabanov, E. B., Colman, S. M., & Escutia, C. (1999). Tectonic and sediment supply control of deep rift lake turbidite systems: Lake Baikal, Russia. *Geology*, *27*(2), 163–166.

Nittrouer, C. A. (1999). STRATAFORM: overview of its design and synthesis of its results. *Marine Geology*, *154*, 3–12.

Normark, W. R., Damuth, J. E., et al. (1997). In R. D. Flood, D. J. W. Piper, A. Klaus, & L. C. Peterson (Eds.), *Sedimentary facies and associated depositional elements of the Amazon Fan* (pp. 611–651). *Proceedings of the ODP, Scientific Research, 155*.

Normark, W. R., & Piper, D. J. W. (1991). Initiation processes and flow evolution of turbidity currents: Implications for the depositional record. In R. H. Osborne (Ed.), *From Shoreline to Abyss; Contribution in Marine Geology in Honor of Francis Parker Shepard* (pp. 207–230). *SEPM (Society for Sedimentary Geology), Special Publication, 46, Tulsa*.

O'Grady, D. B., & Syvitski, J. P. M. (2002). Large-scale morphology of Arctic continental slopes: influence of sediment delivery on slope form. In: Dowdeswell, J. A. and O' Lofaigh, C. (Eds), Glacier-influenced sedimentation on high-latitude continental margins. *Geological Society*, Special Publication 203, 11-31.

Ogston, A. S., Cacchione, D. A., Sternberg, R. W., & Kineke, G. C. (2000). Observations of storm and river flood-driven sediment transport on the northern California continental shelf. *Continental Shelf Research*, *20*(16), 2141–2162.

Parker, G. (1982). Conditions for the ignition of catastrophically erosive turbidity currents. *Marine Geology*, *46*, 307–327.

Parker, G., Fukushima, Y., & Pantin, H. M. (1986). Self-accelerating turbidity currents. *Journal of Fluid Mechanics*, *171*, 145–181.

Parsons, J. D., Bush, J., & Syvitski, J. P. M. (2001). Hyperpycnal flow formation with small sediment concentrations. *Sedimentology*, *48*, 465–478.

Piper, D. J. W., Cochonat, P., Ollier, G., Le Drezen, E., Morrison, M., & Baltzer, A. (1992). Evolution progressive d'un glissement rotationnel en un courant de turbidité: cas du séisme de 1929 des Grands Bancs (Terre Neuve). *Comptes Rendus de l'Academie des Sciences, Paris, 314, Serie II*, 1057–1064.

Piper, D. J. W., & Deptuck, M. (1997). Fine-grained turbidites of the Amazon fan: facies characterization and interpretation. In R. D. Flood, D. J. W. Piper, A. Klaus, & L. C. Peterson (Eds.), *Proceedings of the ODP, Scientific Research, 155* (pp. 79–108).

Piper, D. J. W., & Savoye, B. (1993). Processes of late Quaternary turbidity current flow and deposition on the Var deep-sea fan, north-west Mediterranean Sea. *Sedimentology*, *40*, 557–582.

Praeg, D. B., & Syvitski, J. P. M. (1991). Marine geology of Saguenay Fjord. *Geological Survey of Canada, Open File #2395*.

Pratson, L. F., & Haxby, W. F. (1996). What is the slope of the U.S. continental slope? *Geology*, *24*, 3–6.

Pratson, L., Imran, J., Hutton, E., Parker, G., & Syvitski, J. P. M. (2001). BANG1D: a one-dimensional. Lagrangian model of turbidity current mechanics. *Computers and Geoscience*, *27*(6), 701–716.

Pratson, L. F., Ryan, W. B. F., Mountain, G. S., & Twitchell, D. C. (1994). Submarine canyon initiation by downslope-eroding sediment flows: evidence in late Cenozoic strata on the New Jersey continental slope. *Geological Society of American Bulletin*, *106*, 395–412.

Prior, D. B., Bornhold, B. D., & Johns, M. W. (1986). Active sand transport along a fjord-bottom channel, Bute Inlet, British Columbia. *Geology*, *14*, 581–584.

Prior, D. B., Bornhold, B. D., Wisenam, W. J., Jr, & Lowe, D. R. (1987). Turbidity current activity in a British Columbia fjord. *Science*, *237*, 1330–1333.

Ravenne, C., & Beghin, P. (1983). Apport des expériences en canal à l'interprétation sédimentologique des dépôts de cônes détritiques sous-marins. *Revue de I' Institut Françaisdu Pétrole*, *38*(3), 279–297.

Reed, C. W., Niedoroda, A. W., & Swift, D. J. P. (1999). Modeling sediment entrainment and transport processes limited by bed armoring. *Marine Geology*, *154*, 143–154.

Rigaut, F., (1997). *Analyse et évolution récente d'un système turbiditique méandriforme: l'éventail profond du Zaïre* (209p). PhD Thesis, Univ. Bretagne Occidentale

Rimoldi, B., Alexander, J., & Morris, S. A. (1996). Experimental turbidity currents entering density-stratified water: analogues for turbidites in Mediterranean hypersaline basins. *Sedimentology*, *43*, 527–540.

Savoye, B., & Piper, D. J. W. (1991). The Messinian event on the margin of the Mediterranean Sea in the Nice area, southern France. *Marine Geology*, *97*, 279–304.

Savoye, B., Piper, D. J. W., & Droz, L. (1993). Plio–Pleistocene evolution of the Var deep-sea fan off the French Riviera. *Marine and Petroleum Geology*, *10*, 550–571.

Savoye, B., et al. (2000). Structure et évolution récente de l'éventail turbiditique du Zaïre: premiers résultats scientifiques des missions d'exploration ZAÏANGO. *Comptes Rendus de l'Academie des Sciences, Paris*, *331*, 211–220.

Saint-Onge, G., Mulder, T., Piper, D. J. W., Hillaire-Marcel, C., Stoner, J. S (in press). Earthquake and flood-induced turbidites in the Saguenay Fjord (Québec): a Holocene paleoseismicity record. *Quaternary Science Reviews*.

Schafer, C. T., & Smith, J. N. (1987). Hypothesis for a submarine landslide and cohesionless sediment flows resulting from a 17th century earthquake-triggered landslide in Quebec, Canada. *Geo-Marine Letters*, *7*, 31–37.

Schafer, C. T., Smith, J. N., & Côte, R. (1990). The Saguenay Fiord: a major tributary to the St Lawrence Estuary. In M. I. El-Sabh, & N. Silverberg (Eds.), *Coastal and estuarine studies, 39, Oceanography of a large-scale estuarine system, the St Lawrence* (pp. 378–420). New York: Springer.

Schumm, S. A. (1981). Evolution and response of the fluvial system, sedimentologic implications. In F. G. Ethridge, & R. M. Flores (Eds.), *Recent and ancient nonmarine depositional environments* (pp. 19–29). *Society of Economic Paleontologists and Mineralogists Special Publication, 31*.

Schumm, S. A., & Khan, H. R. (1972). Experimental study of channel patterns. *Bulletin of Geological Society of America*, *88*, 1755–1770.

Scully, M. E., Friedrichs, C. T., & Wright, L. D. (2002). Application of an analytical model of critically stratified gravity-driven sediment transport and deposition from the Eel River continental shelf, northern California. *Continental Shelf Research*, *22*(14), 1951–1974.

Shanmugam, G. (1996). High-density turbidity currents: are they sandy debris flows? *Journal of Sedimentary Research*, *66*, 2–10.

Shepard, F. P., & Dill, R. F. (1966). *Submarine canyons and other sea-valleys*. Chicago: Rand McNally and Co, 381p.

Shepard, F. P., Marshall, N., McLoughlin, P. A., & Sullivan, G. G. (1979). Currents in submarine canyons and other sea valleys. *American Association of Petroleum Geologists, Studies in Geology, no. 8*.

Shepard, F. P., McLoughlin, P. A., Marshall, N. F., & Sullivan, G. G. (1977). Current-meter recordings of low-speed turbidity currents. *Geology*, *5*, 297–301.

Skene, K. I., Mulder, T., & Syvitski, J. P. M. (1997). INFLO1: a model predicting the behaviour of turbidity currents generated at river mouths. *Computers and Geoscience*, *23*(9), 975–991.

Sommerfield, C. K., & Nittrouer, C. A. (1999). Modern accumulation rate and sediment budget for the Eel shelf: a flood-dominated depositional environment. *Marine Geology*, *154*, 227–241.

Sommerfield, C. K., Nittrouer, C. A., & Alexander, C. R. (1999). ^{7}Be as a tracer of flood sedimentation on the northern California continental margin. *Continental Shelf Research*, *19*, 335–361.

Stacey, M. W., & Bowen, A. J. (1988). The vertical structure of density and turbidity currents: theory and observations. *Journal of Geophysical Research*, *93*, 3528–3542.

Stow, D. A. V. (1996). Deep seas. In H. G. Reading (Ed.), *Sedimentary environments: processes, facies and stratigraphy* (pp. 395–453). Oxford: Blackwell Sciences.

Syvitski, J. P. M. (2003). Sediment fluxes and rates of sedimentation. In G. V. Middleton (Ed.), *Encyclopedia of Sediments and Sedimentary Rocks*. Dordrecht, Netherlands: Kluwer, p. 600–606.

Syvitski, J. P. M. (2002). Sediment transport variability in Arctic rivers: Implications for a warmer future. *Polar Research*, *21*(2), 323–330.

Syvitski, J. P. M., & Alcott, J. M. (1993). GRAIN2: prediction of particle size seaward of river mouths. *Computers and Geoscience*, *19*, 399–446.

Syvitski, J. P. M., & Alcott, J. M. (1995). RIVER3: simulation of river discharge and sediment transport. *Computers and Geoscience*, *21*(1), 89–151.

Syvitski, J. P. M., Morehead, M. D., Bahr, D. B., & Mulder, T. (2000). Estimating fluvial sediment transport: the rating parameters. *Water Resources Research*, *36*(9), 2747–2760.

Syvitski, J. P. M., & Schafer, C. T. (1996). Evidence for an earthquake-triggered basin collapse in Saguenay Fjord, Canada. *Sedimentary Geology*, *104*, 127–153.

Tiercelin, J.-J., Cohen, A. S., Soreghan, M., Lezzar, K. E., & Bouroullec, J.-L. (1992). Sedimentation in large rift lakes: example from the Middle Pleistocene—Modern deposits of the Tanganyika Trough, East African Rift System. *Bulletin des centres de Recherche Exploration et Production d' Elf Aquitaine*, *16*, 83–111.

Tiercelin, J.-J., Vincens, A., Barton, C. E., Carbonel, P., Casanova, J., Delibrias, G., Gasse, F., Grosdidier, E., Herbin, J.-P., Huc, A. Y., Jardiné, S., Le Fournier, J., Mélières, F., Owen, R. B., Pagé, P., Palacios, C., Paquet, H., Péniguel, G., Peypouquet, J.-P., Raynaud, J. F., Renaut, R. W., De Renéville, P., Richert, J. P., Riff, R., Robert, P., Seyve, C., Vandenbrouke, M., & Vidal, G. (1987). Le demi-graben de Baringo-Bogoria, Rift Gregory, Kenya 30000 ans d'histoire hydrologique et sédimentaire. *Bulletin des Centres de Recherche Exploration et Production d' Elf Aquitaine*, *11*(2), 249–540.

Traykovski, P., Geyer, W. R., Irish, J. D., & Lynch, J. F. (2000). The role of wave-induced density-driven fluid mud flows for cross-shelf transport on the Eel River continental shelf. *Continental Shelf Research*, *20*(16), 2113–2140.

Weirich, H. (1984). Turbidity currents: monitoring their occurrence and movement with a three-dimensional sensor network. *Science*, *224*, 384–387.

Wheatcroft, R. A., & Borgeld, J. C. (2000). Oceanic flood deposits on the northern California shelf: large-scale distribution and small scale physical properties. *Continental Shelf Research*, *20*, 2163–2190.

Wheatcroft, R. A., Borgeld, J. C., Born, R. S., Drake, D. E., Leithold, E. L., & Nittrouer, C. A. (1997). Rapid and widespread dispersal of flood sediments on the northern California margin. *Geology*, *25*, 163–166.

Wheatcroft, R. A., Borgeld, J. C., Born, R. S., Drake, D. E., Leithold, E. L., Nittrouer, C. A., & Sommerfield, C. K. (1996). The anatomy of an oceanic flood deposit. *Oceanography*, *9*, 158–162.

Wilson, P. A., & Roberts, H. H. (1995). Density cascading: off-shelf sediment transport, evidence and implications, Bahama Banks. *Journal of Sedimentary Research*, *A65*(1), 45–56.

Wright, L. D., Friedrichs, C. T., Kim, S. C., & Scully, M. E. (2001). Effects of ambient currents and waves on gravity-driven sediment transport on continental shelves. *Marine Geology*, *175*, 25–45.

Wright, L. D., Wisenam, W. J., Jr, Bornhold, B. D., Prior, D. B., Suhayda, J. N., Keller, G. H., Yang, Z.-S., & Fan, Y. B. (1988). Marine dispersal and deposition of Yellow River silts by gravity-driven underflows. *Nature*, *332*, 629–632.

Wright, L. D., Wiseman, W. J., Yang, Z.-S., Bornhold, B. D., Keller, G. H., Prior, D. B., & Suhayda, J. N. (1990). Processes of marine dispersal and deposition of suspended silts off the modern mouth of the Huanghe (Yellow River). *Continental Shelf Research*, *10*, 1–40.

Wright, L. D., Yang, Z.-S., Bornhold, B. D., Keller, G. H., Prior, D. B., & Wisenam, W. J., Jr (1986). Hyperpycnal flows and flow fronts over the Huanghe (Yellow River) delta front. *Geo-Marine Letters*, *6*, 97–105.

Zaragosi, S., Eynaud, F., Pujol, C., Auffret, G. A., Turon, J.-L., & Garlan, T. (2001). Initiation of the European deglaciation as recorded in the northwestern Bay of Biscay slope environments (Meriadzek Terrace and Trevelyan Escarpment): a multi-proxy approach. *Earth and Planetary Science Letters*, *188*, 493–507.

Zeng, J., Lowe, D. R., Prior, D. B., Wisenam, W. J., Jr, & Bornhold, B. D. (1991). Flow properties of turbidity currents in Bute inlet, British Columbia. *Sedimentology*, *38*, 975–996.